Somatosensory & Motor Research 1999; 16(2): 69–88

Invited Review

Anatomical loops and their electrical dynamics in relation to whisking by rat

DAVID KLEINFELD, RUNE W. BERG and SEAN M. O'CONNOR

Department of Physics, University of California, La Jolla, CA 92093, USA

Abstract

An accumulation of anatomical, behavioral, and electrophysiological evidence allows us to identify the neuronal circuitry that is involved with vibrissa-mediated sensation and the control of rhythmic vibrissa movement. Anatomical evidence points to a multiplicity of closed sensorimotor loops, while electrophysiological data delineate the flow of electrical signals in these pathways. These loops process sensory input from the vibrissae and send projections to direct vibrissa movement, starting at the level of the hindbrain and proceeding toward loops that involve multiple structures in the forebrain. The nature of the vibrissa-related electrical signals in behaving animals has been studied extensively at the level of neocortical loops. Two types of spike signal are observed that serve as a reference of vibrissa motion: a fast signal that correlates with the relative phase of the vibrissae within a whisk cycle and a slow signal that correlates with the amplitude, and possibly the set-point, of the vibrissae during a whisk. Both signals are observed in vibrissa primary sensory (S1) cortex, and in some cases they are sufficiently robust to allow vibrissa position to be accurately estimated from the spike train of a single neuron. Unlike the case for S1 cortex, only the slow signal has been observed in vibrissa primary motor (M1) cortex. The control capabilities of M1 cortex were estimated from experiments with anesthetized animals in which progressive areas along the vibrissa motor branch were microstimulated with rhythmically applied currents. The motion of the vibrissae followed stimulation of M1 cortex only for rates that were well below the frequency of rhythmic whisking; in contrast, the vibrissae followed stimulation of the facial nucleus, whose cells directly drive the vibrissae, for rates above that of whisking. *In toto*, the evidence implies that there is fast signaling from the facial nucleus, through the mystacial pad and the vibrissae and up through sensory cortex, but only slow signaling at the level of the motor cortex and down through the superior colliculus to the facial nucleus. The transformation from fast sensory signals to slow motor control is an unresolved issue. On the other hand, there is a candidate scheme to understand how the fast reference of vibrissa motion in the whisk cycle may be used to decode the angle of the vibrissae upon their contact with an object. We discuss a circuit in which servo mechanisms are used to determine the angle of contact relative to the preferred phase of the fast reference signals. Support for this scheme comes from results with anesthetized animals on the frequency and phase entrainment of intrinsic neuronal oscillators in S1 cortex. A prediction based on this scheme is that the output from a decoder circuit is maximal when the angle of contact differs from the preferred phase of a fast regerence signal. In contrast, for correlation-based schemes the output is maximal when the angle of contact equals the preferred phase.

Introduction

Spatial navigation requires active sensory as well as motor processes. Animals must extract meaning from the sensory information they amass through their receptors as they search and locomote. A fundamental question in studies of sensory perception is how the blur of sensory input is converted by the nervous systems into a stable perception. Here, we review the question of active sensation in the context of tactile localization of objects accomplished by the exploratory whisking movement of vibrissae in the rat. Our goal is to focus the quest for the algorithm that allows rats to extract a stable image of the world from the input generated by the active movement of their vibrissae. This experimental approach was laid down by Vincent (1912), and was followed, only decades later, by Welker's (1964) study and more contemporary studies that involved trained animals (Hutson and Masterton, 1986; Guic-Robles *et a.l*, 1989,1992; Carvell and Simons, 1990, 1995; Barneoud *et al.*, 1991; Bermejo *et al.*, 1996) and electrophysiological recording (Fee *et al.*, 1997).

Our emphasis is on the structure and function of closed-loop pathways in the sensorimotor vibrissa system that are expected to play an essential role as rats use their vibrissae to search their environment (Fig. 1a). As such, we have organized this review to reflect the following issues: (i) the mechanics of whisking; (ii) the potential involvement of multiple, closed neuronal loops in the sensorimotor pathway; (iii) the nature of exploratory whisking vs tremor motion in sessile animals; (iv) neuronal correlates of

Correspondence: David Kleinfeld, Department of Physics, University of California, 9500 Gilman Drive, La Jolla, CA 92093–0319, USA. Tel: (619) 822–0342; Fax: (619) 534–7697; E-mail: dk@physics.ucsd.edu

0899–0220/99/020069–20

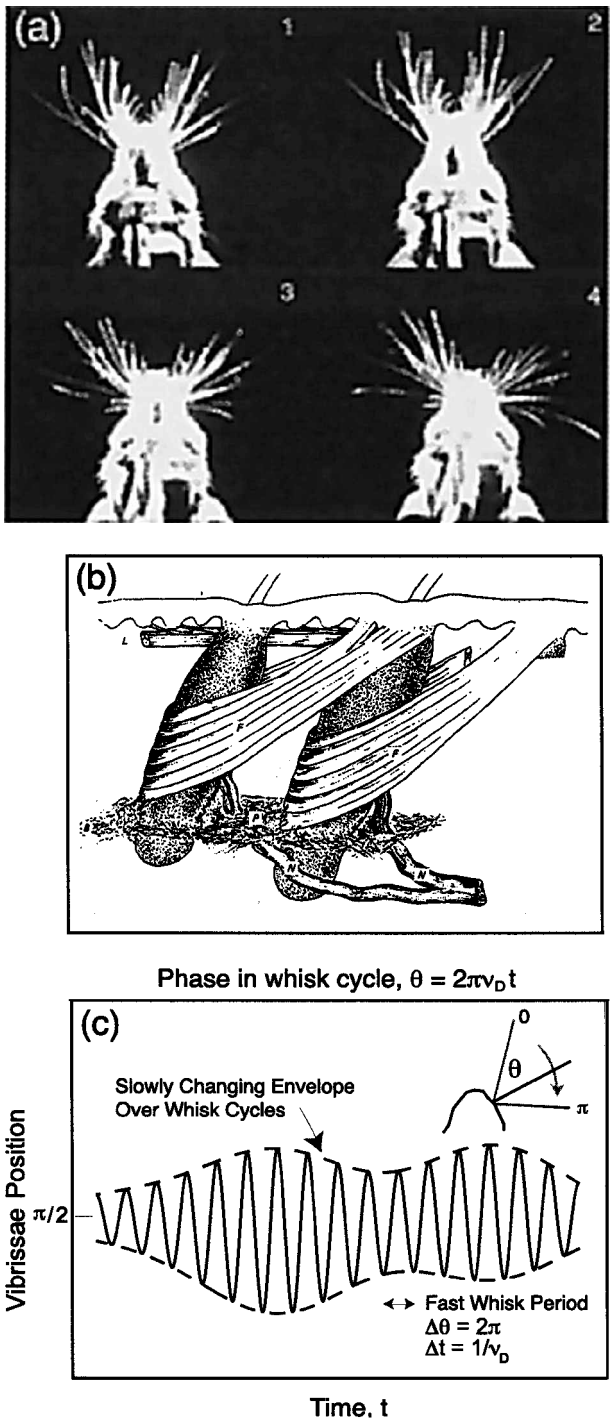

FIGURE 1. The nature and control of exploratory whisking in the rat. (a) Consecutive video frames of the head of a rat as it produces large, exploratory whisks in search of a food tube. The vibrissae were highlighted by strob illumination. The time between frames is 33 ms. (b) The sling-like arrangement of the musculature surrounding each follicle in the mystacial pad. The lower structure is one of two sensory nerves (adapted from Dorfl (1982)). (c) Diagram of the cyclic motion of the vibrissae during exploratory whisking. The animal whisks with frequency ν_D. The set-point and maximum amplitude of the rhythmic whisking vary slowly on the timescale of each whisk cycle.

whisking at the level of sensory and motor cortex; (v) the nature of vibrissa control along the motor pathway; and (vi) mechanisms for computing the position of the vibrissae upon their contact with an object.

Mechanics of whisking

The face of the rat has a muscular thickening, denoted the mystacial pad, that contains upwards of 40 long hairs, referred to as vibrissae, that are nominally arranged in a Manhattan-like grid with five rows. Each vibrissa sits in a follicle that contains sensory nerve endings that originate from a branch of the trigeminal nerve (infraorbital branch of the 5th cranial nerve) (Dorfl, 1985; Rice *et al.*, 1986). The follicle is attached to the mystacial pad near the surface of the skin. This attachment serves as a pivot, and the follicle is propelled by contraction of a muscular sling that is innervated by a branch of the facial nerve (7th cranial nerve) (Fig. 1b) (Dorfl, 1985; Wineski, 1985; Rice *et al.*, 1994). One feature of this arrangement is that protraction is active, while retraction is passive. Thus, the frequency of whisking is ultimately limited by the viscoelastic properties of the mystacial pad. A second feature of this arrangement is that activation of the sensory afferents is expected to depend primarily on a change in the position of the vibrissa relative to that of the follicle, as may occur upon contact of the vibrissae with an external object or during periods of rapid acceleration of the vibrissae in the absence of contact.

The motion of the vibrissae is governed by muscles that move the entire mystacial pad, as well as the muscles that control each follicle (Wineski, 1985). Despite the potential for individual vibrissae to move independent of each other, the vibrissae are observed to move largely as a single unit during a multitude of exploratory behaviors (Vincent, 1912; Wineski, 1983). Further, the vibrissae move with bilateral symmetry (Fig. 1a). Thus, whisking may be described solely in terms of single angle as a function of time, at least to the extent that translational motion of the mystacial pad can be ignored. The change in position is described in terms of a rapidly changing phase within each whisk cycle and a slowly changing set-point and maximum amplitude (Fig. 1c). We will show later that this description allows the position of the vibrissae to be measured via the electromyogram (EMG) at a single location in the mystacial pad.

A final issue concerns the lack of proprioceptive feedback of vibrissa position. In skeletal joints, the extent of muscle contraction is coded by the innervation of specialized muscle fibers, known as spindle fibers, that provide feedback on the actual motion of the muscles as part of a reflex loop. However, there is no evidence for spindle fibers in facial musculature (Bowden and Mahran, 1956). Consistent with this general result, unpublished anatomical studies (F. L. Rice, personal communication) have confirmed the absence of spindle fibers throughout the musculature

of the mystacial pad. Thus, rats must infer the position of their vibrissae through spikes generated by the sensory afferents, a scheme known as peripheral reafference, or by neuronal reference signals that are generated at the central level, a scheme known as corollary discharge.

Anatomical loops in vibrissa sensation and control

A fruitful way to study the gross connectivity within the vibrissa sensorimotor network is in terms of closed loops. The "lowest" of these loops involves only hindbrain structures and is confined to the ipsilateral side of the brain. Higher-order loops involve connections that cross the midline, culminating with loops that involve multiple thalamic and neocortical areas. By tracing through closed pathways that involve the vibrissae, we hope to illustrate the relevant anatomy while keeping a focus on the possible neuronal computations and behavioral functions that are enabled by this closed-loop system. Note that for the benefit of readability, the references that established the connectivity among different loci are listed in the figure captions.[1]

Hindbrain loop

The most compact sensorimotor loop involves input that is relayed by the trigeminal ganglion to trigeminal nuclei, that in turn project to the facial motor nucleus, which drives the vibrissae (Fig. 2). Projections from the neurons of the trigeminal ganglion have peripheral branches that innervate the vibrissa follicles and have central branches that project to trigeminal nuclei, which include the principal sensory nucleus and the three spinal nuclei, denoted oralis, interpolaris, and caudalis; these projections form several somatotopic representations of the ipsilateral vibrissae. The trigeminal nuclei project to the lateral subnucleus of the ipsilateral facial nucleus; this subnucleus sends motor output to the mystacial pad to complete the loop. The observed pattern of connectivity suggests that the trigeminal nuclei may exert feedback control on whisking. However, there are presently no data that show direct connections between vibrissa trigeminal afferents and the facial motor neurons that drive the vibrissae.

Of critical importance, whisking occurs in the absence of sensory feedback. Welker (1964) observed bilateral whisking in animals with a unilateral lesion of the trigeminal nerve, and more recently Ziegler reported (personal communication) highly coherent bilateral whisking in animals with bilateral lesions. These data imply that a yet undiscovered central pattern generator[2] drives rhythmic whisking, a hypothesis first suggested in this context by Carvell *et al.* (1991).

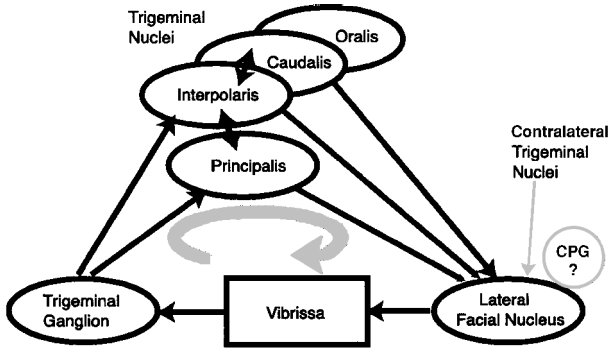

FIGURE 2. Hindbrain-level sensorimotor loop. (**vibrissae → trigeminal ganglion**) The vibrissae are innervated by two kinds of sensory afferents that originate from the infraorbital nerve (Vincent, 1913; Dorfl, 1985; Rice *et al.*, 1986). (**trigeminal ganglion → trigeminal nuclei**) Sensory input from the trigeminal ganglion enters the hindbrain at the trigeminal nuclei, consisting of the principal sensory nucleus (PrV) and the spinal trigeminal nuclei denoted oralis (SpVO), interpolaris (SpVI), and caudalis (SpVC) (Cajal, 1911; Torvik, 1956; Clarke and Bowsher, 1962). The PrV and SpVI nuclei and the magnocellular portion of SpVC have somatotopic maps of the vibrissae ("barrelettes") (Ma and Woolsey, 1984); SpVO also receives sensory input from the vibrissae yet does not contain a map (Belford and Killackey, 1979a, b). Lastly, there is high internuclear connectivity, especially among SpVC and SpVO (Jacquin *et al.*, 1990a). (**trigeminal nuclei → facial nucleus**) The facial nucleus contains five subnuclei, of which the lateral subnucleus is involved in vibrissa control (Papez, 1927; Martin and Lodge, 1977). Vibrissa areas of the trigeminal nuclei SpVC, PrV, and SpVI connect to the lateral subnucleus, primarily through ipsilateral projections. The dominant projection appears to arise from the magnocellular portion of SpVC (Erzurumlu and Killackey, 1979; Isokawa-Akesson and Komisaruk, 1987). (**facial nucleus → vibrissae**) The facial nucleus sends projections to the papillary muscles surrounding each vibrissa (Arvidsson, 1982; Dorfl, 1982, 1985; Rice and Arvidsson, 1991). The lateral subnucleus of the facial nucleus contains a somatotopic map of the vibrissae (Martin and Lodge, 1977).

Midbrain loop

A higher-level loop incorporates the superior colliculus and includes connections that cross the midline (Fig. 3). The superior colliculus is a laminar, midbrain structure, with each layer nominally devoted to integrating sensory and motor information relevant to a particular sensory modality (Stein *et a.l*, 1975). In the rat, the intermediate and deep layers of the colliculus appear to be devoted to somatic sensorimotor processing, with the more rostral and lateral areas responding to vibrissa input (Huerta *et al.*, 1983; Isokawa-Akesson and Komisaruk, 1987; Miyashita *et al.*, 1994). The middle and deep layers of the rostral–lateral aspects of the superior colliculus receive vibrissa-related inputs from the contralateral trigeminal nuclei, and descending afferents from the superior colliculus project to the lateral subnucleus of the contralateral facial nucleus. An additional input that converges to the same laminae

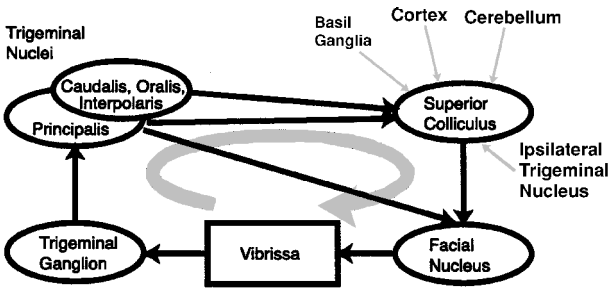

FIGURE 3. Midbrain-level sensorimotor loop. (**trigeminal nuclei → superior colliculus**) The trigeminal nuclei project to vibrissa somatotopic areas of the superior colliculus (Drager and Hubel, 1976; Killackey and Erzurumlu, 1981; Huerta *et al.*, 1983; Steindler, 1985; Bruce *et al.*, 1987; Jacquin *et al.*, 1989; Benett-Clarke *et al.*, 1992). The connection from interpolaris appears to be the strongest (Killackey and Erzurumlu, 1981; Huerta *et al.*, 1983; Jacquin *et al.*, 1989), while that from caudalis is problematic (Killackey and Erzurumlu, 1981). All connections terminate in the intermediate and deep layers, and tend to occur in the lateral and rostral aspects of the colliculus (Huerta *et al.*, 1983). The projections from the trigeminal ganglia to the colliculus are likely to be collaterals of projections to the thalamus (Mantle-St. John and Tracey, 1987; Benett-Clarke *et al.*, 1992). (**superior colliculus →facial nucleus**) The intermediate and deep layers of the colliculus project to the lateral subnucleus of the facial nerve nucleus (Isokawa-Akesson and Komisaruk, 1987; Miyashita *et al.*, 1994; Miyashita and Shigemi, 1995).

arises from ipsilateral vibrissa M1 cortex. Yet the computations that the colliculus performs on the confluence of vibrissa sensory inputs and motor commands are presently unknown.

Cerebellar loops that involve trigeminal nuclei and the colliculus

The pontine-cerebellar system appears to function as a hindbrain-level intermediary in a loop that involves indirect connections between the contralateral trigeminal nuclei and the ipsilateral superior colliculus (Fig. 4). The trigeminal nuclei project to both the pons and the inferior olive, which in turn directly project to the cerebellum; similar inputs, which project to the same crura in cerebellum, arise from the intermediate and deep layers of the superior colliculus. The cerebellar Purkinje cells synapse on the cerebellar nuclei, and this provides output projections to superior colliculus to complete the loop.

Beyond the issue of loops that directly involve the vibrissae, it has been proposed that the embedded loop between the pontine-cerebellar system and the superior colliculus (Fig. 4) may function as a rhythmic pattern generator (Westby *et al.*, 1993).[3] This pattern generator would not depend on the integrity of the trigeminal sensory input and thus could function as the central pattern generator that drives rhythmic vibrissa motion by the facial nucleus.

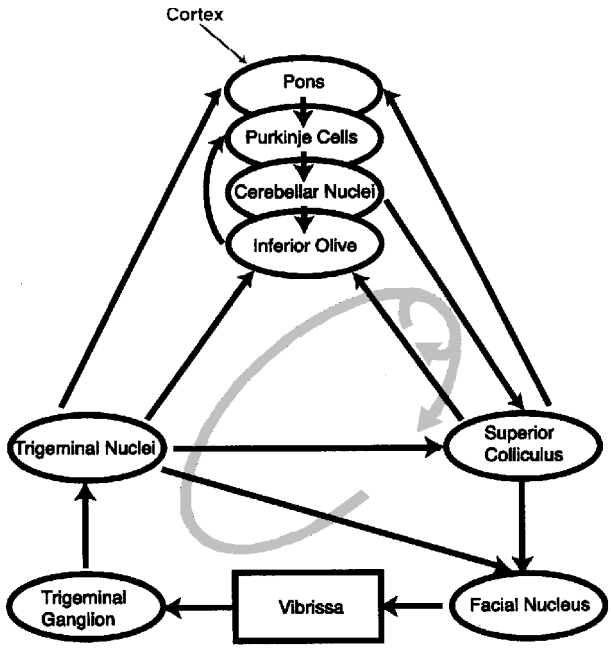

FIGURE 4. Midbrain-level sensorimotor loops, including projections with cerebellar nuclei. (**trigeminal nuclei → cerebellum**) The trigeminal nuclei provide vibrissa sensory input to the cerebellum via two paths: interpolaris and caudalis project via the inferior olive climbing fibers (Huerta *et al.*, 1983; Jacquin *et al.*, 1989) and principalis, interpolaris and caudalis project via pontine mossy fibers (Smith, 1973; Watson and Switzer, 1978; Huerta *et al.*, 1983; Swenson *et al.*, 1984; Steindler, 1985; Mantle-St. John and Tracey, 1987). Projections from the trigeminal nuclei to the inferior olive overlap those from the olive to the cerebellum (Huerta *et al.*, 1983); the target areas in the cerebellum include crura I and II (Watson and Switzer, 1978; Huerta *et al.*, 1983) and the paramedian lobule and uvula (Watson and Switzer, 1978), all areas with facial receptive fields. (**superior colliculus → cerebellum**) The colliculus sends projections to the cerebellar cortex, including target areas crura I and II, through both the inferior olive and the pons (Kassel, 1980). (**cerebellum → superior colliculus**) The deep cerebellar nuclei send a projection to the colliculus (Lee *et al.*, 1989; Westby *et al.*, 1993, 1994), which forms a "colliculus → cerebellum → colliculus" loop.

Thalamic forebrain loop

Multiple structures in ventral and dorsal thalamus receive input from the trigeminal nuclei. Only one of these, zona incerta in the ventral thalamus, projects directly back to the superior colliculus (Fig. 5), where it forms inhibitory connections with the superior colliculus. Thus, the zona incerta appears to function as a forebrain-level intermediary in a loop that involves the trigeminal nuclei and the colliculus.

Cortical forebrain loops

These high-level loops are formed by projections that involve multiple thalamic nuclei and cortical areas. The thalamocortical branch of the sensorimotor pathway involves projections from the trigeminal

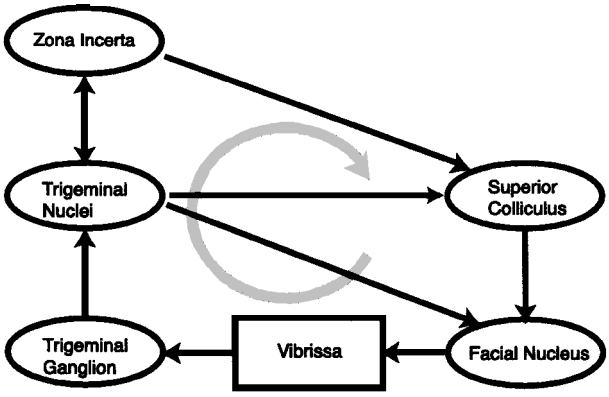

FIGURE 5. Forebrain-level sensorimotor loop that projects directly to the midbrain. This loop contains a single forebrain structure, the zona incerta. (**trigeminal ganglion →zona incerta**) An excitatory projection (Nicolelis *et al.*, 1992; Kolmac *et al.*, 1998). (**zona incerta → trigeminal ganglion**) An inhibitory connection (Nicolelis *et al.*, 1992; Kolmac *et al.*, 1998). (**zona incerta → superior colliculus**) An inhibitory connection (Kim *et al.*, 1992; Nicolelis *et al.*, 1992).

nuclei to thalamic nuclei, from thalamus to sensory areas and then motor areas in cortex, and from motor cortex down to the superior colliculus to complete a loop (Fig. 6). Two pathways dominate the synaptic input of vibrissa sensory information to cortex (see Diamond (1995) and Keller (1995) for reviews of corticothalamic connectivity). The principal trigeminal nucleus projects to the ventral posteromedial nucleus of dorsal thalamus (lemniscal path), which in turn has major projections to vibrissa S1 cortex and minor projections to secondary sensory cortex. The spinal trigeminal nuclei project to the posterior nucleus of dorsal thalamus (paralemniscal path), which in turn projects to vibrissa primary and secondary cortices. Additional thalamic input to S1 cortex arises from the zone incerta, both directly via inhibitory projections and indirectly through projections to dorsal thalamus. Lastly, there are extensive reciprocal, intercortical projections among primary, secondary and posteroventral sensory cortices and motor cortices (Fabri and Burton, 1991a; Keller, 1993).

The loops comprising thalamic and cortical forebrain structures are closed in at least two ways (Fig. 6).[4] Vibrissa S1 cortex sends descending projections to the superior colliculus, which completes the loop through hindbrain and midbrain structures (Fig. 3). The dominant descending pathway, however, encompasses the intercortical projection from vibrissa S1 to M1 cortex. Vibrissa M1 cortex sends descending projections to the superior colliculus that, as in the case of the descending projections from S1 cortex, complete a loop. Importantly, the descending projection from M1 cortex has been shown to directly overlap with neurons in superior colliculus that project to the vibrissa region of the facial nucleus.

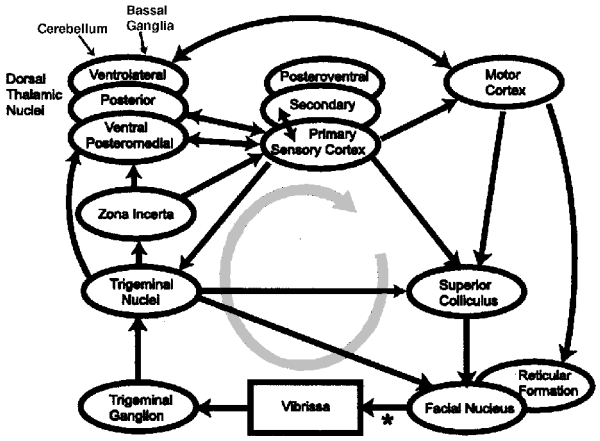

FIGURE 6. Forebrain-level sensorimotor loop. The * indicates the facial motor nerve, transiently blocked with a nerve cuff in the experiments of Fee *et al.* (1997). (**trigeminal nuclei → thalamus**) All trigeminal nuclei send projections to the ventral posteromedial (VPM) and posterior (POm) nuclei in the dorsal thalamus (Lund and Webster, 1967; Smith, 1973; Erzurumlu and Killackey, 1980; Mantle-St. John and Tracey, 1987; Hoogland *et al.*, 1987; Jacquin *et al.*, 1989; Killackey *et al.*, 1990; Chiaia *et al.*, 1991a; Benett-Clarke *et al.*, 1992; Diamond *et al.*, 1992; Nicolelis *et al.*, 1992; Williams *et al.*, 1994). The representation of the vibrissae forms a somatotopic map ("barreloids") in VPM (Van Der Loos, 1976; Sugitani *et al.*, 1990) and POm (Nothias *et al.*, 1988; Fabri and Burton, 1991b). (**zona incerta → thalamus**) Zona incerta, in the ventral thalamus, projects to the VPM and POm nuclei in the dorsal thalamus (Power *et al.*, 1999). (**thalamus ↔cortex**) Thalamic regions VPM, POm, and zona incerta project to primary (S1), secondary (S2) and posterior ventral areas of sensory cortex and the cortex sends feedback projections to VPM, POm and the trigeminal nuclei (Wise and Jones, 1977; Donoghue *et al.*, 1979; Donoghue and Kitai, 1981; Hoogland *et al.*, 1987; Carvell and Simons, 1987; Koralek *et al.*, 1988; Welker *et al.*, 1988; Jacquin *et al.*, 1990b; Chiaia *et al.*, 1991a, b; Diamond *et al.*, 1992; Nicolelis *et al.*, 1992; Deschênes *et al.*, 1996; Lévesque *et al.*, 1996). The projection from zona incerta to cortex is unique in providing an inhibitory input (Chapin *et al.*, 1990; Nicolelis *et al.*, 1992). (**intercortical**) Vibrissa S1 cortex forms reciprocal projections with other vibrissa sensory areas (Carvell and Simons, 1987; Chapin *et al.*, 1987; Welker *et al.*, 1988; Fabri and Burton, 1991a) and with vibrissa motor cortex (White and deAmicis, 1977; Asanuma and Keller, 1991; Fabri and Burton, 1991a; Aroniadou and Keller, 1993; Keller, 1993; Miyashita *et al.*, 1994; Izraeli and Porter, 1995). The representation of the vibrissae forms a somatotopic map in S1 (Woolsey *et al.*, 1974; Durham and Woolsey, 1977) ("barrels"), and S2 (Carvell and Simons, 1986; Kleinfeld and Delaney, 1996) cortices. Note that the primary motor cortex is taken as the parasagittal agranular medial area. (**cortex → superior colliculus**) Both sensory and motor cortex send descending projections to the superior colliculus (Wise and Jones, 1977; Killackey and Erzurumlu, 1981; Welker *et al.*, 1988; Mercier *et al.*, 1990). Miyashita and Shigemi (1995) have demonstrated possible cellular interaction between the descending cortical M1 projection to colliculus and the colliculus to facial nucleus projection, consistent with the relay of motor commands to the facial nucleus. (**M1 → superior colliculus**) A direct connection from the vibrissa motor cortex to an unidentified nucleus in the reticular formation adjacent to the facial nucleus (Miyashita *et al.*, 1994) is suggestive of a central pattern generator (CPG; Fig. 2), in analogy with the CPG for mastication (Nozaki *et al.*, 1986).

Vibrissa M1 cortex sends a direct projection to an undefined nucleus in the reticular formation adjacent to the facial nucleus (Fig. 6). A likely candidate is the parvicellular reticular formation, which lies dorsal to the facial nucleus and forms direct projections to the facial nucleus (Mogoseanu *et al.*, 1994). This target is an additional candidate for the central pattern generator that drives rhythmic whisking, much as mastication is driven by a pattern generator in the reticular nuclei (Nozaki *et al.*, 1986).

Spike signals in primary cortex during whisking

All of the published studies to date in awake and either behaving or attentive animals have been at the level of cortex (Carvell *et al.*, 1996; Fee *et al.*, 1997), although other studies on recordings from both subcortical and cortical areas are in progress (Goldreich *et al.*, 1997; Moxon *et al.*, 1998; Sachdev *et al.*, 1998). Part of the bias toward cortex undoubtedly reflects the ease of access to cortical areas across the lissencephalic brain of the rat. However, justification for this bias is also derived from the results of behavioral experiments with decorticate animals. Animals that are devoid of primary vibrissa cortex can reorient in response to vibrissa stimulation, but fail depth perception tasks that involve the use of the vibrissae (Hutson and Masterton, 1986; Barneoud *et al.*, 1991).

EMG as a behavioral measure

The motor output of interest in the study of the vibrissa sensorimotor system is the angle of the vibrissae as a function of time (Fig. 1c). While this position may be extracted from high-speed video images, the scalar nature of vibrissa motion during exploratory whisking (Fig. 1a) suggests that a single measure of the activity of the mystacial musculature may serve as an accurate correlate of vibrissa position. One such measure is the EMG, in which electrodes imbedded in the mystacial pad are used to record the high-frequency spike activity of the musculature (Carvell *et al.*, 1991). This signal is rectified and low-pass filtered to yield the extent of electrical activation of the mystacial muscles (Kamen and Caldwell, 1996); we denote this processed signal the EMG.[5] Increases in the amplitude of the EMG correspond to protraction of the vibrissae, while decreases correspond to retraction (Fig. 7a).

The EMG measured during exploratory whisking contains bouts of rhythmic activity that span 1 or more seconds, as illustrated by the epoch between 2 and 4 s in Figure 7a. The period of these oscillations is relatively constant throughout the bout, but the envelope surrounding the oscillations is seen to vary, albeit smoothly, over the course of the bout. The fast oscillations, with a spectral peak near 8 Hz (Fig. 7b), correspond to the rhythmic motion of the vibrissae. The slowly varying envelope, with spectral components below 5 Hz, contains contributions from both changes in the maximum amplitude of the whisk and changes in the midpoint of the vibrissae. The latter correspondence is illustrated by the data of Carvell *et al.* (1991), who simultaneously measured the mystacial EMG and the position of the vibrissae via video images and showed that the midpoint of the position determined by the two methods largely track each other (Fig. 7c).

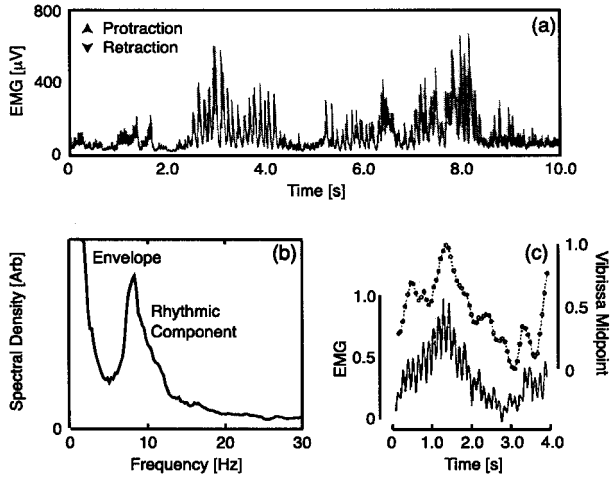

FIGURE 7. The electromyogram (EMG) of the mystacial pad and its relation to vibrissa motion. (a) A single record of the EMG that illustrates two bouts of whisking during an exploratory task (Fig. 1a). Note the fast oscillations and the slowly varying envelope of the oscillations. The amplitude of the EMG is maximum at protraction, corresponding to contraction of the mystacial muscles (Fig. 1a), and minimum at retraction, which is passive. The EMG was recorded with a 50 μm diameter tungsten wire that was implanted in the mystacial pad. The raw signal was amplified, half-wave rectified and integrated with a 4-pole Bessel low-pass filter set at 200 Hz. (b) The spectral density of the EMG as a function of frequency. Note the peak at 8 Hz, which corresponds to the frequency of rhythmic whisking, and the spectral energy at low frequencies, which corresponds to changes in the envelope of this positive definite signal. The spectral estimate was based on ~ 1000 s of data. (c) Relation of the set-point of vibrissa motion, determined from the analysis of video images, to the envelope of the EMG record. The midpoint is the angle about which the vibrissae oscillate ((c) is adapted from Carvell *et al.* (1991)).

Two forms of rhythmic whisking: basic phenomenology

Rats perform at least two forms of rhythmic whisking that are correlated with their overall behavioral state (Semba and Komisaruk, 1984; Fee *et al.*, 1997). One form occurs while the animals are immobile and corresponds to low amplitude, tremor-like movements of the vibrissae, also referred to as "twitching" (Nicolelis *et al.*, 1995). These motions are distinguished by a relatively low amplitude EMG signal, with spectral components between 7 and 11 Hz, and highly synchronous cortical activity, as inferred from the synchrony of the electrocorticogram (ECoG) (Fig. 8a). The second form occurs while animals

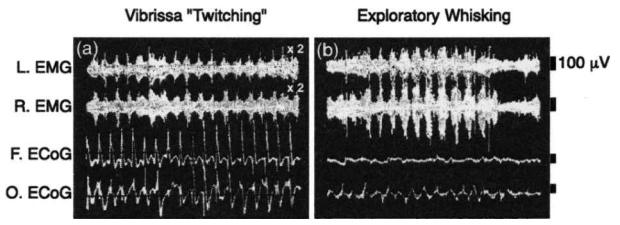

FIGURE 8. Vibrissa and cortical activity during two types of whisking. (a) The tremor, or vibrissa "twitching" state. Note the relatively low amplitude of the right (R) and left (L) electromyograms (EMGs) and the high degree of cortical synchrony in the frontal (F) and occipital (O) electrocorticograms (ECoG). (b) The exploratory whisking state. Note the relatively high amplitude EMG and the loss in cortical synchrony (adapted from Semba and Komisaruk (1984)).

actively explore their environment and correspond to large amplitude motion of the vibrissae, such as those illustrated in Figure 1a. These motions are distinguished by a relatively high amplitude EMG signal, with spectral components between 6 and 9 Hz, and largely asynchronous cortical activity (Fig. 8b).

Responses in vibrissa sensory cortex during vibrissa "twitching"

Chapin, Nicolelis, and coworkers (Nicolelis *et al.*, 1995, 1997) devised a strategy to simultaneously record unit activity from multiple regions along the vibrissa sensory branch in rats, as well as measure the motion of their vibrissae with video techniques, as the animals rested between periods of exercise. They observed highly coherent oscillatory spike activity across multiple sites in vibrissa S1 cortex, as well as sites in the principal and spinal trigeminal nuclei (PrV and SpV, respectively, in Figure 9a) and in dorsal thalamus (VPM in Figure 9a). The phase of the oscillations was relatively uniform both within and between brain regions, such that most of the variance of these responses was accounted for by the first principal component of the temporal response (Fig. 9a). Further, the responses were time-locked to low amplitude tremor movements of the vibrissae (Fig. 9b). Thus all units in primary vibrissa cortex have a similar preferred phase within the whisk cycle for spiking.

The nature of the cortical activity and the large coherence of this activity with the vibrissa movement are reminiscent of the "tremor" state described by Semba and Komisaruk (1984) (Fig. 8a). The brain activity in this state is thought to be dominated by thalamocortical oscillations, variously described as "high-voltage spindles" (Buzsaki, 1991) or absent seizures (Steriade *et al.*, 1993; McCormick and Bal, 1997). The data of Nicolelis *et al.* (1995) are remarkable in that they show that such coherent activity extends to subthalamic areas. However, as

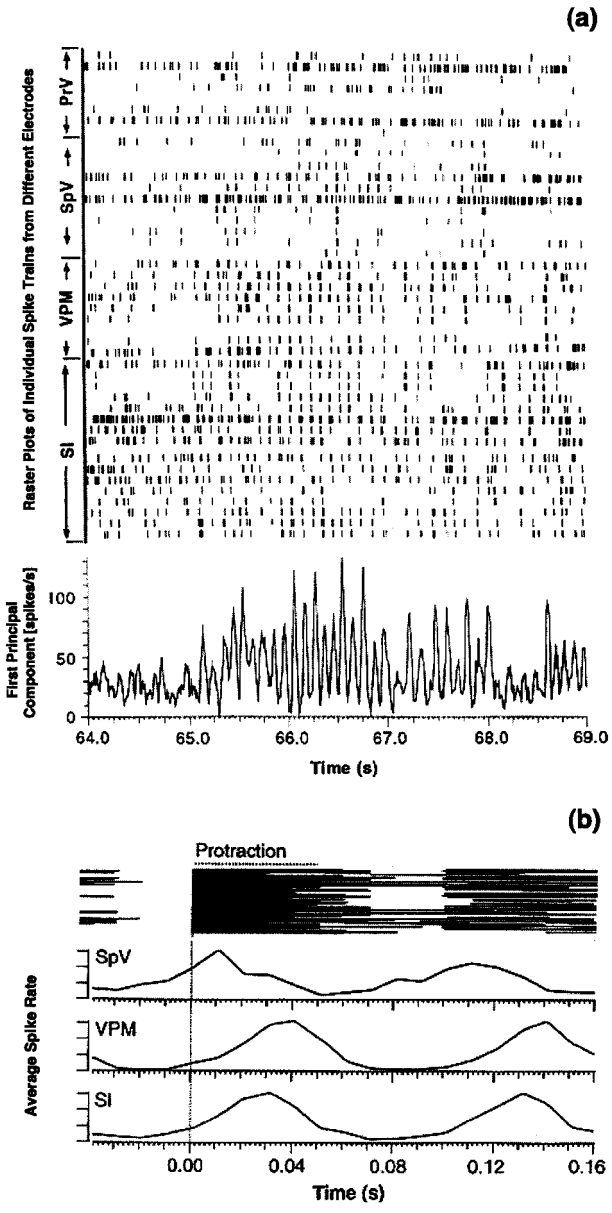

FIGURE 9. Simultaneously recorded brain activity from multiple sites in the brainstem trigeminal nuclei (PrV, principal trigeminal nucleus; SpV, spinal trigeminal nuclei), thalamus (VPM, ventral posterior medial nucleus of dorsal thalamus) and vibrissa primary sensory (S1) cortex during epochs of vibrissa "twitches". (a) Single-trial spike rasters plots from separate extracellular units, grouped according to anatomical area, for a particular 5 s interval. The lower, smooth trace is the first principal component of the raster responses, defined as the leading eigenvalue of the covariance matrix that is formed by summing the outer products of the individual responses (Ahmed and Rao, 1975). (b) The relation of vibrissa position, determined from video images, to the time- and site-averaged spike responses. Note that the spike activity in each region has, on average, a single preferred phase in the whisk cycle (adapted from Nicolelis *et al.* (1995)).

the vibrissa sensorimotor pathway forms a closed loop (Fig. 6), it is impossible to determine if the oscillatory activity in the trigeminal nuclei results from feedback connections from higher areas or from peripheral reafference.

Single-unit responses in vibrissa sensory cortex during exploratory whisking

We now turn to an understanding of the spike trains in vibrissa S1 cortex during an exploratory whisking task. Fee *et al.* (1997) devised a paradigm in which rats were trained to perch on a ledge and whisk in search of a food tube. The rats performed this task with blindfolds on, during which time they whisked over large angles for epochs of ~ 5 s (Fig. 1a). The positions of the vibrissae were inferred from measurements of the EMG. Extracellular signals were simultaneously recorded from multiple sites in S1 cortex during the whisking epochs, from which single-unit spike trains (Fee *et al.*, 1996) as well as local field potentials (LFP) were derived. No significant correlation between the spike trains recorded from different locations was found and, as discussed in detail later (Fig. 13), the LFP was featureless during the epochs of whisking. The large rhythmic whisking motions and the asynchronous extracellular activity imply that the animal is in the "exploratory whisking" state of Semba and Komisaruk (1984) (Fig. 8b).

Fee *et al.* (1997) found a significant correlation between the occurrence of a spike and the phase of the vibrissae within the whisk cycle (Fig. 1c), as illustrated by the three examples in Figure 10a. Importantly, different units tended to spike at different phases, so that each unit could be associated with a preferred phase. This is in contrast to the case of vibrissa "twitching", in which all units tended to fire at the same phase (near full protraction; Fig. 9b). The distribution of the modulation depth and the phase of the correlation over all measured units shows that the values of preferred phase are uniformly represented, but that there is a tendency for the modulation depth to be greatest for units whose preferred phase corresponds to protraction from the retracted position (Fig. 10b).

The above results show that spike activity is correlated with relative position within the whisk cycle. Fee *et al.* (1997) also found significant correlations between the envelope of the rhythmic whisking epochs (Fig. 1c) and the single-unit spike trains. The envelope was found by demodulating the EMG near the whisking frequency (insert, Fig. 11), so that the values of the envelope correspond to the amplitude of the rhythmic whisking motion. The distribution of amplitudes at all time points was compared with the distribution of amplitudes at times when a spike occurred. For the example of Figure 11, we observe a significant decrement in the occurrence of a spike at small amplitudes of the EMG, with a concomitant enhancement at large amplitudes. Overall, relative enhancement or suppression of the spike rate at large whisking amplitude occurred with essentially equal probability. There was no obvious relationship between the degree of amplitude coding (Fig. 11) and phase modulation

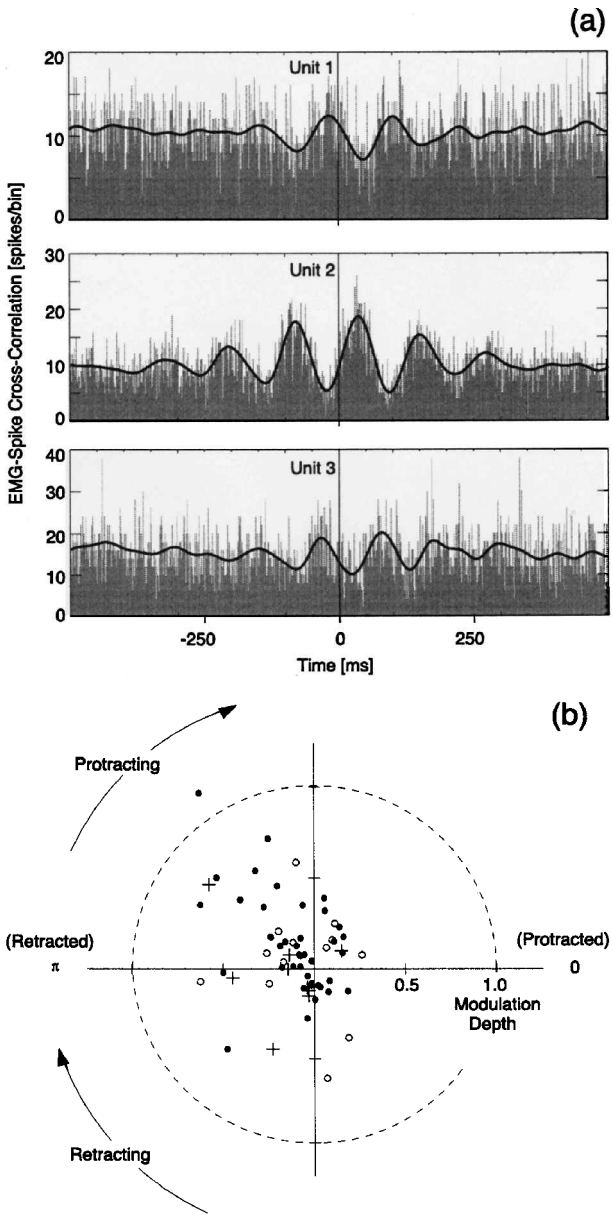

FIGURE 10. Relation of single-unit spike activity in vibrissa S1 cortex to vibrissa position. (a) Correlations between three simultaneously recorded units and the electromyogram (EMG). The correlations were calculated as spike averages triggered off the positive peak of the EMG. Note that the phase is different for each unit. The modulation depth of the correlation is defined as the peak-to-peak amplitude divided by the baseline spike rate, equal to that at long lag times. The phase corresponds to 2π-times the time-lag to the peak in the correlation, divided by the period of the oscillation. (b) Polar plot of the modulation depth and preferred phase for 115 units across three animals; different symbols refer to different rats. Note that all preferred phases are represented (adapted from Fee *et al.* (1997)).

(Fig. 10) among the single units in these experiments.

How well can vibrissa position, as inferred from the EMG signal, be predicted from the spike train of a single unit? The linear transfer function that predicts the EMG signal from the spike train was

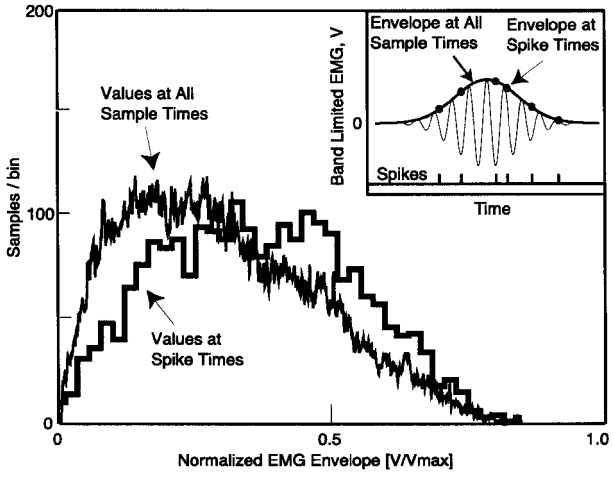

FIGURE 11. Relation between the amplitude of the whisk cycle and probability of spiking for a particular single unit in vibrissa S1 cortex. The amplitude of the electromyogram (EMG) envelope, denoted V, is sampled at each time point (insert; the solid line indicates the envelope and the dots denote values of the envelope that coincide with a spike). We plot the number of occurrences of the value of the EMG envelope at all times (Values at All Sample Times) and at times when a spike occurred (Values at Spike Times). The difference between the two curves results from a correlation between EMG amplitudes and the probability of spiking. The significance of the difference is established by a Kolmogorov–Smirnov test (adapted from Fee *et al.* (1997)).

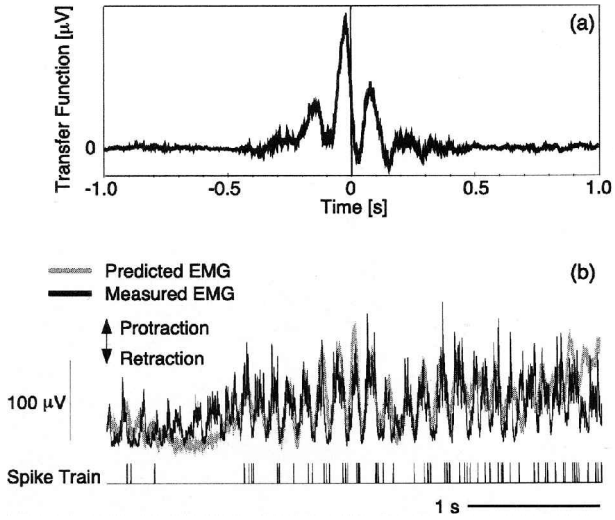

FIGURE 12. The transfer function, or linear predictor of the electromyogram (EMG) from the measured spike train. (a) Plot of the linear predictor calculated as a least-squares estimator over 19 of 20 trials of simultaneously recorded spike trains and EMGs. Note that the transfer functions decay in about one whisk period. (b) Comparison between the measured EMG and the predicted EMG, calculated as a convolution of the transfer function in part (a) with the measured spike train. The predicted EMG signal is seen to coincide well with the measured signal; a region of poor prediction at the beginning of the trial coincides with the unit not firing ((b) is adapted from Fee *et al.* (1997)).

calculated as an average over all but one trial for a particular data set (Fee *et al.*, 1997). The transfer function shows damped oscillations near the whisk frequency (Fig. 12a). When applied to the spike train of the excluded trial, the predicted EMG signal appears to coincide well with the measured signal (Fig. 12b). The ability to predict the EMG from spike trains implies that the output of some units has both a sufficiently high probability of spiking and a sufficiently strong correlation with the EMG so as to represent vibrissa position on a real-time basis.

We now consider the direction of signal flow in the forebrain sensorimotor loop (Fig. 6). The correlates of vibrissa position in S1 cortex may originate either from peripheral reafference or discharge along a central pathway, e.g., feedback from vibrissa M1 cortex. To determine the pathway(s), Fee *et al.* (1997) used a transient block to the facial nerve to "open" the sensorimotor loop (⋆ in Fig. 6). The animals continued to whisk on their ipsilateral side during the block; the normally high coherence between whisking on both sides of the face allowed the ipsilateral EMG to serve as the measured reference of vibrissa position. The conclusion from these manipulations was that the fast correlate of vibrissa position (Fig. 1c), which reports the phase of the whisk cycle (Fig. 10) and varies on the 1–10 ms timescale, originates via peripheral reafference. In contrast, the slow correlate of vibrissa position (Fig. 1c), which reports the amplitude of the whisk (Fig. 11) and varies on the 0.1–1 s timescale, originates from a corollary discharge.

Two forms of rhythmic whisking: correspondence with synchronous vs asynchronous activity in S1 cortex

In the course of the exploratory whisking experiments (Figs. 10–12), there were epochs of time in which the animals rested before resuming the task. During the rest period, the behavior of the rat alternated between immobility and exploration. We focus on the record of Figure 13. In the early part of the record, the state of the animal included epochs of strong LFP activity near 10 Hz, which were always accompanied by vibrissa "twitches" and weak EMG activity, as well as epochs of asynchronous LFP activity, some of which were accompanied by epochs of a strong EMG (Spindling or Whisking; Fig. 13). A protracted period of synchronous LFP activity coincided with the appearance of weak vibrissa "tremors" (Spindling; Fig. 13). Lastly, there was a complete absence of synchronous LFP activity, but the appearance of a strong EMG signal at the whisk frequency, as the animal performed the task (Exploratory Whisking Task, Fig. 13). These data imply that the two forms of whisking (Semba and Komisaruk, 1984), "twitches" (Figs. 8a and 9) vs exploration (Figs. 1, 8b, and 10–12), coincide with mutually exclusive states of cortical activation.

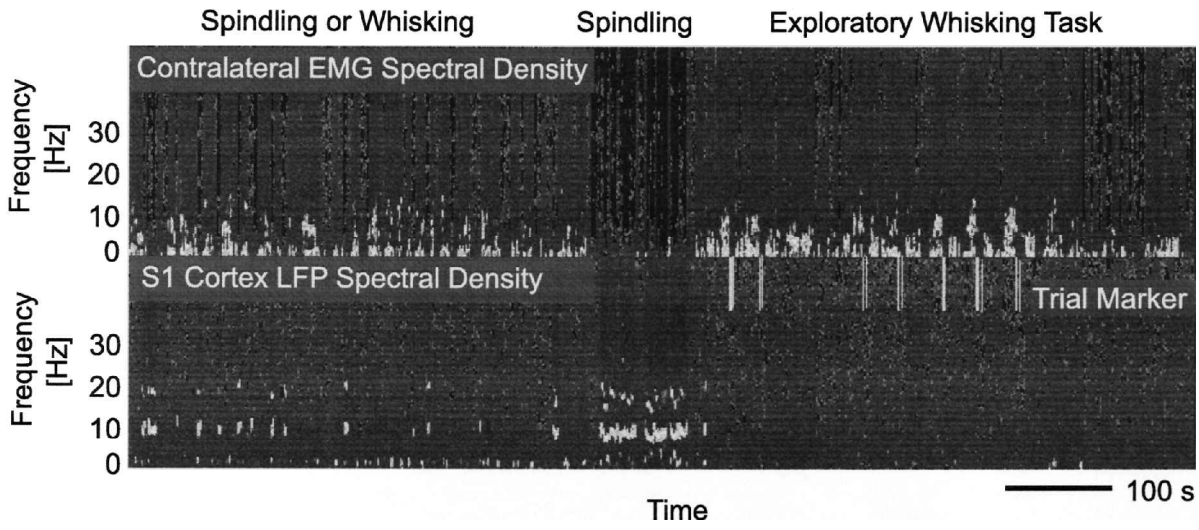

FIGURE 13. Relation of cortical synchrony to the electromyogram (EMG) during immobile vs exploratory states in the rat. The top spectrogram is the power density in the EMG vs frequency and time. A strong peak in the spectrogram near 10 Hz coincides with exploratory whisking, while a weak or undetectable peak coincides with immobility, including epochs of vibrissa "twitches". Note that increased power density is coded by lighter shades of gray. During the epoch labeled "Spindling", the vibrissae were observed to make fine tremor, or "twitch", movements (video data not shown). The behavioral markers during the interval marked "Exploratory Whisking Tasks" indicate when the animal successfully completed the search task with its vibrissae. The bottom spectrogram is the power density in the local field potential (LFP). Note that a peak in this spectrogram coincides with synchronous electrical activity in S1 cortex. Such a peak occurs during spindling but not during exploratory whisking, consistent with the data in Figure 7.

Single-unit responses in vibrissa motor cortex during whisking

Vibrissa primary motor cortex forms extensive, reciprocal projections with S1 cortex (Fig. 6). *A priori*, these connections could lead to shared information about actual and intended vibrissa position. To measure the cortical correlates of vibrissa position in M1, Carvell and coworkers (1996) devised a paradigm in which gentled but otherwise naive rats were enticed to whisk in response to an attractive odorant. The whisks encompassed large angles and were sustained for epochs of ~ 1–5 s. The position of the vibrissae were inferred from measurements of the EMG and extracellular signals were recorded from sites in M1 cortex during the whisking epochs (Fig. 14a). Carvell *et al.* (1996) observed that, unlike the case of vibrissa S1 cortex (Fig. 10), there were no strong correlations of unit output with the rhythmic whisking pattern.[6] In contrast, as in the case of vibrissa S1 cortex (Fig. 11), Carvell *et al.* (1996) found a strong correlation between unit activity and the envelope of EMG activity (Fig. 14b). In these measurements, the envelope contained contributions from both a change in set-point of the vibrissae and a change in the amplitude of the whisk.

Transfer functions for rhythmic signaling along the motor branch

The results of Carvell *et al.* (1996) imply that the fast cortical reference signal of vibrissa position (Fig. 10) is not transmitted between S1 and M1 cortices, despite the direct connections between these areas and the ability of even layer 1 intercortical connections to drive spiking in neurons throughout the target column (Nakajima *et al.*, 1988; Cauller and Connors, 1994). One question suggested by this result concerns the nature of neuronal control signals along the motor branch of the sensorimotor pathway (Fig. 6), i.e., M1 $\rightarrow$ superior colliculus $\rightarrow$ facial nucleus $\rightarrow$ vibrissae. We thus consider preliminary data (R. W. Berg and D. Kleinfeld, unpublished) on the temporal response properties along this branch. The approach in these experiments was to quantify the movement of the vibrissae that was elicited by repetitive microstimulation of different brain regions in the anesthetized animal.

Microstimulation was used to activate a brain region with a train of pulsed constant-current stimuli. The trains were constructed so that a single stimulus could elicit vibrissa motion (see legend to Figure 15), as described in mapping studies based on microstimulation (Hall and Lindholm, 1974; Gioanni and Lamarche, 1985; Neafsey *et al.*, 1986; Donoghue and Sanes, 1988; Sanes *et al.*, 1990; Miyashita *et al.*, 1994; Weiss and Keller, 1994). The motion of the vibrissae was monitored magnetically (Fig. 15a). We calculated the value of the transfer function between the repetitive stimuli and the measured motion of the vibrissae at the stimulation frequency.

We observed that, at the level of the facial nucleus, the vibrissae could accurately follow stimulation up to a roll-off of ~ 12 Hz (Fig. 15b), above the ~ 8 Hz frequency of exploratory whisking (Fig. 7b). In

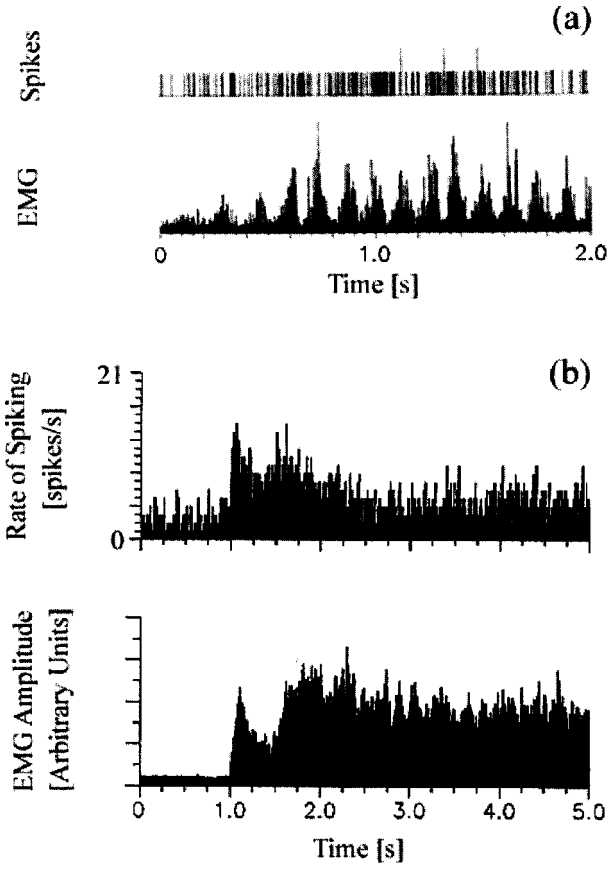

FIGURE 14. Relation of unit spike activity in vibrissa M1 cortex to vibrissa position. (a) Simultaneous records of a single-trial spike train and the concomitantly recorded electromyogram (EMG). Here, as in all cases, there is no obvious correlation between the occurrence of a spike and the amplitude of the EMG. (b) Plots of the trial-averaged spike response for a particular unit and the average EMG. The averages were aligned to start 1.0 s before the onset of whisking. Note the clear correlation between the rate of spiking and the value of the EMG (adapted from Carvell *et al.* (1996)).

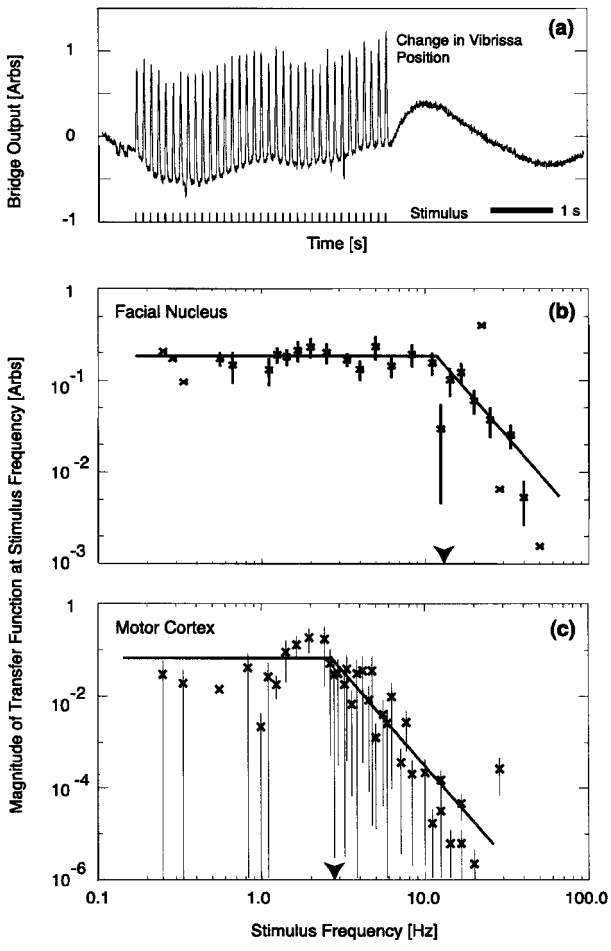

FIGURE 15. Preliminary data on the ability of the vibrissae to follow rhythmic stimulation of different areas in the motor branch of the sensorimotor loop. Long Evans female rats were anesthetized with ketamine/xylazine (0.005% (w/w) and 0.0015% (w/w), respectively) and held stereotaxically. Constant-current stimuli (suprathreshold, unipolar, 200 μs wide pulses of 10–50 μA that were repeated five times at 2 ms intervals) were delivered through tungsten microelectrodes (1–2 MΩ at 1 kHz). Vibrissa position was determined electronically by detecting the motion of a small magnet glued to the principal vibrissa with a magnetoresistive bridge. The magnet, plus extra glue to stiffen the shaft, increased the moment of inertia of the vibrissa by ~ 50%. We calculated the transfer function between a train of stimuli and the vibrissa motion for a range of stimulation frequencies; the transfer function was typically statistically significant at the stimulation frequency and at its harmonics. (a) Trace of the position of a vibrissa as the facial motor nucleus was stimulated at a repetition rate of 8.3 Hz. (b) Plot of the magnitude of the transfer function at the value of the stimulation frequency, as a function of stimulation frequency, for the ipsilateral facial motor nucleus. Note the onset of roll-off near 15 Hz (arrow head), with slope f^{-2}. The bars are one standard deviation, calculated as a trial-to-trial average. (c) Bode plot of the magnitude of the transfer function at the stimulation frequency for the contralateral vibrissa M1 cortex. Note the onset of roll-off near 3 Hz (arrow head), with slope f^{-4}.

contrast, at the level of M1 cortex, the vibrissae could follow stimulation only up to a roll-off of ~ 3 Hz (Fig. 15c), well below the frequency of exploratory whisking. An intermediate frequency response was observed at the level of the superior colliculus (data not shown). These results imply that M1 cortex cannot control vibrissa position of the fast timescale of the whisk cycle, but can control motion on longer timescales. One caveat is that the timescales may be different in awake, attentive animals, particularly at the level of M1 cortex.

Timescales of signaling in the sensorimotor loop

The electrophysiological data on the sensory and motor branches of the vibrissa sensorimotor loop (Figs. 10, 11, 14, and 15) can be combined with the anatomical structure of the forebrain loop (Fig. 6) to yield an overview of signal flow (Fig. 16). We observe fast signaling that starts at the facial nucleus and courses through the vibrissae and up through the trigeminal pathway to thalamus and S1 cortex. The addition of a slow signal that correlates with the

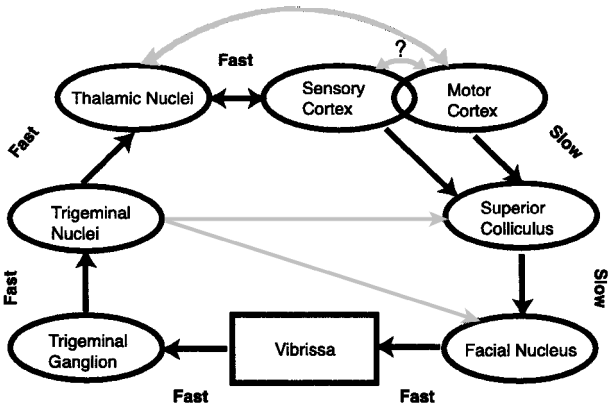

FIGURE 16. Summary schematic of the timescale of signaling along the sensorimotor loop that involves the cortex (Fig. 6). The dark arrows correspond to pathways that were directly or indirectly probed as part of the studies reviewed here. Specifically, fast signaling of vibrissa position through the sensory branch is known from direct measurements with anesthetized and sessile animals (trigeminal ganglion (Simons *et al.*, 1990); trigeminal nuclei (Nicolelis *et al.*, 1995); thalamic nuclei (Carvell and Simons, 1987; Diamond *et al.*, 1992; Nicolelis *et al.*, 1993, 1995); S1 (Welker, 1976; Simons, 1978; Armstrong-James and Fox, 1987; Armstrong-James *et al.*, 1992; Nicolelis *et al.*, 1995) and, by inference from the presence of a fast cortical correlate of vibrissa position in S1 (Fee *et al.*, 1997) (Figs. 8–10). Slow signals of vibrissa amplitudes were established in S1 and M1 from measurements with awake animals (Carvell *et al.*, 1996; Fee *et al.*, 1997) (Figs. 11 and 14). Slow control signaling along the motor branch, including M1 and the superior colliculus, is implied by the results of microstimulation experiments (Fig. 15). Similarly, fast control of vibrissa position by the facial nucleus was established by microstimulation experiments (Fig. 15). The light gray arrows refer to major paths in the sensorimotor loop with uncharacterized signaling properties.

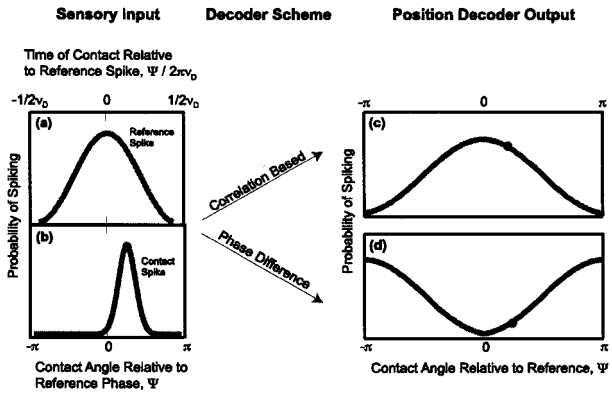

FIGURE 17. Diagram of decoding schemes to extract the relative phase of the vibrissae upon their contact with an object. (a) The probability of a unit in S1 producing a spike for whisking in air. This tuning curve defines the preferred angle for the fast reference signal (Fig. 10). (b) The probability of a unit in S1 producing a spike upon contact of the vibrissa with an object. It is assumed that the contact occurs at an angle Ψ relative to the preferred angle. The free whisking frequency is ν_D. (c and d) The spiking output as a function of contact angle relative to the preferred angle for different decoding schemes. The scheme in (c) is based on the correlation of the two inputs and produces a maximal output when contact occurs at the preferred angle of the reference signal. The scheme in (d) is based on a phase comparison of the two inputs and produces a minimal output at the preferred angle and a maximal output away from the preferred angle of the reference signal.

envelope of rhythmic whisking is manifest by S1. Slow signaling is manifest along the motor branch, down to the level of the facial nucleus, to complete the loop. At present it is unknown if the slow cortical reference signals for vibrissa position that are observed in S1 and M1 cortices are, in fact related, although the central origin of the slow signal in S1 (Fee *et al.*, 1997) suggests that that may be so. Further, it is unknown if and how the fast and slow signals interact in the sensation of objects by the vibrissa, as may be posited to occur in S1.

Detection of vibrissa contact

We shift our focus and consider how the rat may determine the angle of the vibrissa, relative to the orientation of the mystacial pad, upon their contact with an object. A central and yet unresolved issue is whether the output of neurons in S1 is "tuned" to the position of the vibrissa during contact. In other words, does the probability that a unit may spike upon contact vary as a function of the angle of the vibrissae in the whisk cycle? To the extent that activation of the sensory afferent depends on a change in the position of a vibrissa relative to that of its follicle (Fig. 1b), we assume for purposes of discussion that activation is equally likely at all angles in the whisk cycle. The issue then becomes one of deducing the angle of contact under two assumptions: (i) a neuron may fire at a preferred phase of the whisk cycle in the absence of contact, to form a reference signal (Fig. 17a; see also Figure 10b); and (ii) a neuron may spike upon contact with an object during any phase of the whisk cycle (Fig. 17b).

There are two general classes of decoding schemes for reconstructing the phase of the vibrissae upon contact with an object. In the first class, the output is *maximal* when the equal-time correlation between the two sensory signals is maximal, i.e., when the phase of contact is close to that of the reference signal (Fig. 17c). This scheme may be implemented in a variety of functionally equivalent ways (Kam *et al.*, 1975). In one realization, the inputs from the two sensory signals are summed and the sum causes a neuronal decoder to fire only if it exceeds a judiciously set threshold value. In another, the sensory inputs are multiplied (Koch and Poggio, 1992) and the product modulates the output of a neuronal decoder. In the second class of decoding schemes, the output is *minimal* when the phase-shift between the two sensory signals is zero, i.e., when the phase of contact is close to that of the reference signal (Fig. 17d). This scheme

occurs naturally in phase-sensitive detection and is discussed in detail below. We emphasize the dramatic and experimentally testable difference in the predictions between these two classes of decoding scheme; one yields a maximal signal at the preferred reference phase of neurons in S1 while the other yields a minimal signal (c.f. Figs. 17c, d).

Phase-sensitive detection of vibrissa contact

Ahissar *et al.* (1997) addressed the question of how vibrissa contact is coded by neurons in S1 cortex. They presented evidence that this sensory process may involve a phase-sensitive servo mechanism to extract the position of the vibrissae upon their contact with an object (Fig. 17d).

We consider first a brief tutorial on the use of phase-sensitive detection to lock the frequency of an interval oscillator with that of an external, rhythmic input (de Bellescize, 1932). A phase-sensitive servo consists of two parts that are connected by a feedback loop (Fig. 17a): (i) an input controlled oscillator, which may be an intrinsic neuronal oscillator, whose frequency is monotonically shifted by an external rhythmic input; and (ii) a comparator that generates an output signal that is proportional to the difference in timing of the intrinsic neuronal oscillator and that of an oscillatory external signal. The output from the comparator may need to be filtered, depending on the details of the servo, and is used as an error signal to shift the frequency of the intrinsic neuronal oscillator so that it matches the frequency of the external reference signal.[7] The error signal is a sensitive indicator of changes in the timing, both in frequency and phase, of the input.

In steady state, the frequency of the intrinsic neuronal oscillator, denoted ν_R, is locked to the frequency of a rhythmic external drive, denoted ν_D, that is applied to the vibrissae, i.e.,

$$\nu_R = \nu_D. \qquad \text{(Eqn 1)}$$

Even though the frequencies are locked, there may be a constant difference in the timing between the intrinsic neuronal oscillator and the external drive. This is expressed in terms of the phase difference, ϕ, between the output of the two oscillators, i.e.,

$$\phi = f^{-1}\left\{\frac{\nu_D - \nu_R^{free}}{G}\right\} + 2\pi\nu_D(\tau_D - \tau_R) \qquad \text{(Eqn 2)}$$

The first term in eqn 2 is a function of the error signal from the comparator, denoted $f(x)$, which depends on the frequency of the external rhythmic input relative to the natural frequency of the intrinsic neuronal oscillator, ν_R^{free}, and on the gain of the intrinsic neuronal oscillator, G (Fig. 18a). The second term is a function solely of signal delays, where τ_D is the peripheral delay, taken as $\tau_D = 10$ ms

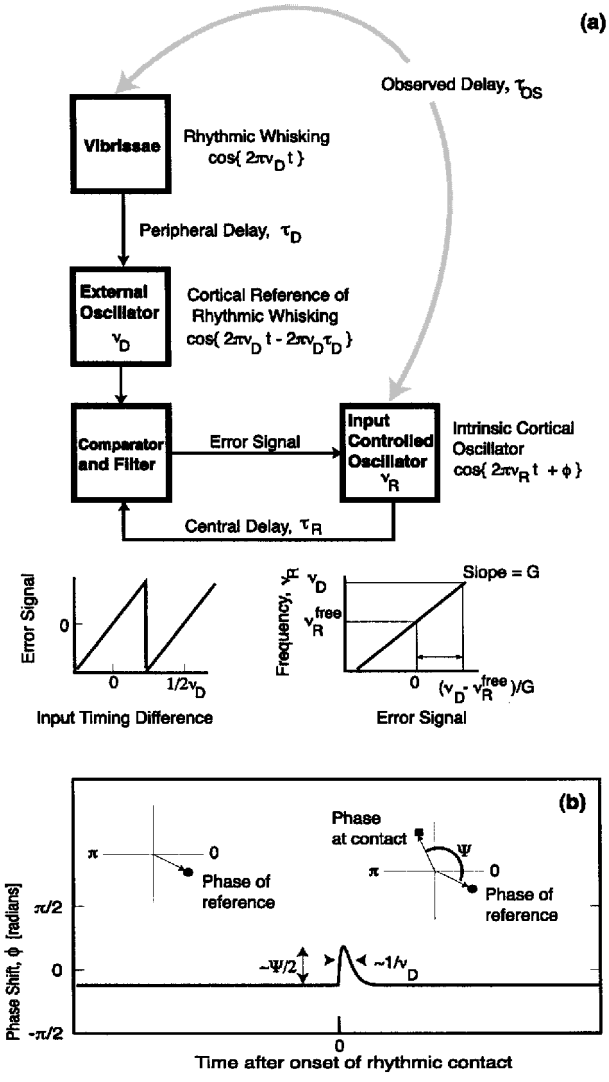

FIGURE 18. Model, and predictions based on the model, for a neuronal phase-sensitive servo mechanism. (a) Schematic of a servo that includes major delays in signaling. A comparator and filter generates a slowly varying output (error signal) that is a function of the difference in timing between input from the cortical reference of rhythmic whisking (with drive frequency ν_D) and the intrinsic cortical oscillator (with frequency $\nu_R = \nu_R^{free} + G$ (error signal)). For consistency with the experimental data (Fig. 19c), we consider a comparator whose error signal is a periodic function of the input timing difference with a frequency of $2\nu_D$. Note that the observed delay between the intrinsic cortical oscillations and the rhythmic drive to the vibrissae, τ_{OS}, includes contributions from peripheral delays, τ_D, and central delays, τ_R, intrinsic to the servo. (b) Diagram that illustrates how the phase of the intrinsic neuronal oscillator is transiently modulated upon contact with an object during rhythmic whisking. Prior to contact the reference of rhythmic whisking occurs at a fixed phase. Upon contact of the vibrissae with an object, at an angle of just over $\pi/2$ in the diagram, the phase of the external rhythmic reference is shifted as spikes occur at both the cortical reference position and on contact with an object. The change in average angle leads to a transient shift in the phase of the intrinsic cortical oscillator that depends on the phase of contact relative to the preferred phase for the cortical reference, i.e., Ψ in the diagram (see also Figure 17d). An alternative servo scheme is given by Ahissar *et al.* (1997).

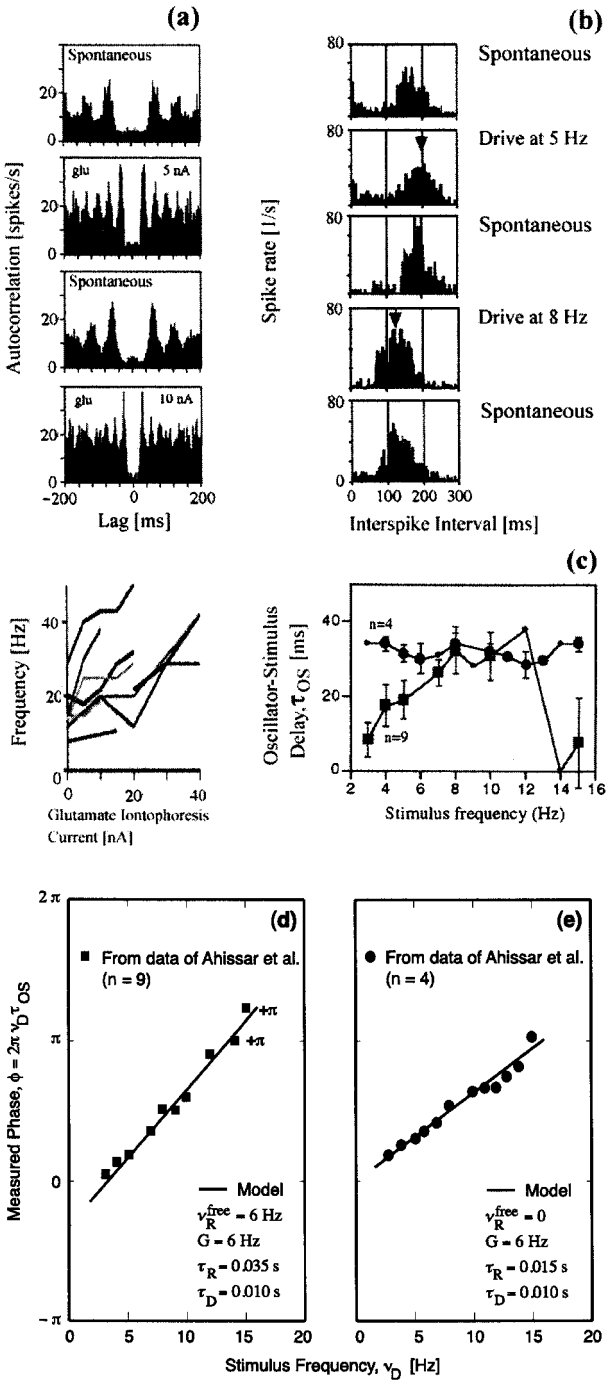

FIGURE 19. Data and analysis in support of a model for phase-sensitive detection of rhythmic drive of the vibrissae. (a) Intrinsic neuronal oscillators in vibrissa S1 cortex that shift their frequency in the presence of iontophoretically applied glutamate. Shown are the autocorrelation functions for spontaneous activity (panels 1 and 3) and activity in the same unit in response to glutamate (panels 2 and 4); glutamate is seen to raise the frequency of the oscillatory firing. The summary plot shows that, in general, the firing rate is monotonically increased in the presence of this transmitter. (b) Evidence that the intrinsic neuronal oscillators can frequency lock to rhythmic stimulation of the vibrissae. Shown are the interspike interval distributions during spontaneous activity (panels 1, 3 and 5) and the change in these distributions in response to external vibrissa stimulation at 5 Hz (panel 2) and 8 Hz (panel 4). Note that the frequency remains partially entrained after removal of the stimulus (c.f., panels 2 and 3, and 4 and 5). (c) The time delay, τ_{OS}, between the onset of external stimulation and that of spiking in the intrinsic oscillators. The data were pooled into two populations based on the nature of the response. Note the apparent reset in the delay for the major population near a stimulus frequency of 13 Hz. (d and e) The measured time delays in (c) are replotted as phase vs frequency. Note the offset of two points in (d) by the addition of a phase of $+\pi$ radians. The solid line is a fit to eqn 2 with $f(x) = x$ and parameters indicated in the figure. The periodicity of π radians in the data of (d) suggests that the output of the comparator (Fig. 18a) has a periodicity of $1/2\nu_D$, as opposed to $1/\nu_D$ for data with a periodicity of 2π radians ((a)–(c) are adapted from Ahissar *et al.* (1997)).

(Armstrong-James *et al.*, 1992), and τ_R is a central delay.

One function of a phase-sensitive servo is to generate a transient change in the error signal from the comparator when the phase of the input is changed. This will occur when the vibrissae contact an object during rhythmic whisking, as illustrated in Figure 18b, and thus the phase-sensitive servo provides a mechanism to explain the "phasic" on- and off-responses of neurons. Prior to contact, the phase of the external rhythmic input is constant, as in Figure 9a. Upon contact of the vibrissae with an object, the phase of the rhythmic whisking reference is shifted as spikes occur at both a reference position and at object contact within the whisk cycle. This leads to a transient shift in the phase of the intrinsic neuronal oscillator (Fig. 18b). The duration of this transient is expected to be at least as great as the inverse of the oscillation frequency, i.e., $1/\nu_D$ or hundreds of milliseconds. The amplitude of the transient is minimal if contact occurs at the preferred phase of the reference signal and increases as contact occurs before or after the preferred phase (Figs. 17d and 18b).

Cortical units that behave as intrinsic neuronal oscillators in the absence of sensory input were

demonstrated in anesthetized animals by Dinse *et al.* (1992). Ahissar *et al.* (1997) recorded the extracellular spike signal from similar units and showed that the frequency of the oscillations, which ranged between 5 and 10 Hz in the absence of external input, is monotonically increased by the local application of glutamate, an excitatory neurotransmitter. The shift in frequency was reversible and observed across all cells tested (Fig. 19a). These cells satisfy the role of intrinsic neuronal oscillators whose frequency may be monotonically shifted.

Neurons that serve as reporters of a rhythmically varying external reference signal were described by Fee *et al.* (1997) (Fig. 10a)[8]. Neurons that compare the timing of signals from an intrinsic neuronal oscillator in cortex (Fig. 18a) with that of a reference of vibrissa motion remain unidentified (Simons and Hartings, 1998), although work in progress (Ahissar and Haidarliu, 1998) suggests that such neurons may lie in the posterior nucleus of dorsal thalamus, consistent with the slow signaling in the paralemniscal path (Diamond *et al.*, 1992). Nonetheless, Ahissar *et al.* (1997) found that the output of the intrinsic neuronal oscillators they identified (Fig. 19a) would frequency lock to a rhythmic drive applied to the vibrissae (Fig. 19b). The time delay between the intrinsic neuronal oscillators and the external drive to the vibrissae, τ_{OS} (Fig. 18a), was not constant, as expected for units that are solely driven by an outside stimulus (circles; Fig. 19c), but varied systematically with the frequency of the rhythmic drive (squares; Fig. 19c). This variation is a signature of a phase-sensitive servo. In fact, these data are well fit by a straight line when replotted as phase ($\phi = 2\pi\nu_D\tau_{OS}$; Fig. 19d). The slope and intercept of this line are accounted for by reasonable parameters in the model (eqn 2 with, for simplicity, $f(x) = x$; Fig. 19d); similar parameters accounted for the units that were solely driven by outside stimulation (Fig. 19e).

The good fit between the data and a straight line predicted by the model (eqn 2) is enticing, but serves only as a consistency argument based on data largely from anesthetized animals. The validity of the phase-sensitive model as the mechanism used by the forebrain to compute vibrissa position relative to the mystacial pad awaits further experimental evidence, particularly with regard to the identification of candidates for the comparator circuit and the nature of the output from these circuits (Fig. 17d).

Concluding remarks

Extensive anatomical studies have shown that the circuitry involved in the vibrissa sensorimotor system is configured as a series of closed loops (Figs. 2–6, 16). These anatomical studies suggest the need for electrophysiological measurements that delineate the functional roles of the pathways. At the level of the hindbrain (Fig. 2), the trigeminal nuclei provide a link between sensory input and motor control. It will be instructive to determine if there is a sensory-mediated control of motor output at the level of the "vibrissa $\rightarrow$ trigeminal ganglia $\rightarrow$ trigeminal nucleus $\rightarrow$ facial nucleus $\rightarrow$ vibrissa" loop, possibly through simultaneous recordings from the trigeminal and facial nuclei during a behavior task. A second issue is to identify the putative central pattern generator of rhythmic whisking.

At the level of the midbrain (Fig. 3), the superior colliculus receives convergent inputs via trigeminal, thalamic, cortical, basal ganglion, and cerebellar pathways (Figs. 4–6), and is thus positioned to integrate direct and indirect sensory channels with motor commands. Despite this rich convergence of pathways, there is a dearth of information on signaling in this structure in the awake rat. The presence of closed-loop connections between the superior colliculus and cerebellar nuclei (Fig. 4) raises the further possibility that feedback between the superior colliculus and the cerebellum could form a central pattern generator for rhythmic whisking; simultaneous measurements of olivary oscillations and whisking may settle this issue. Lastly, the role of the pontine-cerebellar pathway (Fig. 4) in mediating the behavior of animals in response to vibrissa contact is unexplored, although experiments on the lick response in rats (Welsh *et al.*, 1995) suggest the strong involvement of cerebellar nuclei.

Multiple thalamic and cortical structures are involved in forebrain pathways that merge vibrissa sensory input with motor control (Figs. 5 and 6), and the results of behavioral experiments imply that this pathway must be intact for animals to pair a sensory input with a learned percept (Hutson and Masterton, 1986). The issue of how animals compute the absolute position of their vibrissae, as a step toward constructing a stable percept of objects in their environment, has been only partially addressed. On the one hand, the spike trains of some units in vibrissa S1 cortex accurately code vibrissa position in a single trial (Fig. 12). On the other hand, there is incomplete evidence as to how the rat uses this information. In the scheme of Ahissar *et al.* (1997), the rat computes the angle of vibrissa contact based on the relative timing between the reference signal and that caused by contact (Figs. 17d, 18 and 19). Alternatively, the sensitivity of cortical units could vary as a function of their angle in the whisk cycle, in analogy with position preference in the visual system (Andersen and Mountcastle, 1983) (Fig. 17d). It should be possible to distinguish among these possibilities by recording from animals as their vibrissae are perturbed at different angles in the whisk cycle during an exploratory whisking task.

The experimental evidence shows that the representation of vibrissa position in cortex involves both fast signals, which can vary on the 10 ms timescale and report the phase of the vibrissae within a whisk cycle (Fig. 10), and slow signals, which vary on the

1 s timescale and report the amplitude and/or set-point of the whisk (Figs. 11 and 14). The fast signal originates from peripheral reafference, but it is unknown how such reafference results in different units spiking at different phases in the whisk cycle. The slow signal originates centrally, but the source of this signal and the possible relation of this signal to the fast reference, is unknown. It is tempting to speculate that a phase-sensitive servo is a link between the fast and slow cortical reference signals, so that the output of a comparator, i.e., an error signal (Fig. 18a), is the slow cortical reference signal that correlates with the set-point of the vibrissa (Figs. 7 and 14). This correspondence implies that the frequency of exploratory whisking will change as the animal changes its set-point, e.g., as it protracts its vibrissae to palpate an object; the behavioral data of Carvell and Simons (1990) are consistent with this idea.

Acknowledgements

This article is based on material presented at "Barrels XI". We thank Ford Ebner for suggesting the topic of the presentation. We further thank Michale Fee for contributing to the data in Figures 7 and 13, Suri Venkatachalam for contributing to the data in Figure 15, Ehud Ahissar, James Bower, John Chapin, Asaf Keller, and Daniel Simons for pertinent discussions, Beth Friedman and two anonymous referees for their comments on an earlier version of the manuscript, and the Whitehall Foundation for their support.

Notes

1. Anatomical abbreviations. Hindbrain: TG, trigeminal ganglion; TN, trigeminal nuclei, including PrV, principalis, SpVO, oralis, SpVI, interpolaris, SpVC, caudalis; FN, facial nucleus. Midbrain: SC, superior colliculus. Thalamic nuclei: VPM, ventral posteromedial; POm, posterior; ZI, zona incerta; VL, ventral lateral. Cortex: S1, primary sensory; S2, secondary sensory; PV, posteroventral; M1, primary motor cortex.
2. The central pattern generator hypothesis, derived primarily from experimental evidence gathered with invertebrates and subcortical vertebrate preparations, states that rhythmic motions are controlled by autonomous neuronal circuits, albeit circuits whose output may be gated or modulated by extrinsic inputs (Kleinfeld and Sompolinsky, 1988; Getting, 1989).
3. For completeness, we note that the basal ganglia also form a closed loop with the superior colliculus. The colliculus sends projections to the basal ganglia (Tokuno *et al.*, 1994), and the basal ganglia send inhibitory connections to the colliculus (Faull and Mehler, 1978; Gerfen *et al.*, 1982; Westby *et al.*, 1993, 1994; Niemi-Junkola and Westby, 1998); the role of the basal ganglia in whisking is presently unclear.
4. We note two additional loops at the level of the forebrain. One involves projections between the forebrain and the cerebellum. Vibrissa S1 cortex sends descending projections to the pons (Kennedy *et al.*, 1966; Wise and Jones, 1977; Shambes *et al.*, 1978; Wiesendanger and Wiesendanger, 1982a, b; Welker *et al.*, 1988; Mercier *et al.*, 1990) whose climbing fiber input to the cerebellum overlaps with that from the trigeminal nuclei (Bower *et al.*, 1981; Morisette and Bower, 1996). Vibrissal M1 cortex also projects to the pons (Wiesendanger and Wiesendanger, 1982a, b; Miyashita *et al.*, 1994). Feedback to cortex occurs via projections from the deep cerebellar to ventral lateral thalamic nuclei (Haroian *et al.*, 1981; Gerfen *et al.*, 1982; Deniau *et al.*, 1992; Middleton and Strick, 1997). The second loop involves projections from vibrissa S1 and M1 cortices to basal ganglia (Wise and Jones, 1977; Donoghue and Kitai, 1981; Mercier *et al.*, 1990; Lévesque *et al.*, 1996). Feedback to cortex occurs via ventral lateral thalamus, as in the case of cerebellar feedback (Fig. 6).
5. The definition of the EMG is ambiguous in the literature. Some authors refer to the unprocessed signal of muscular spikes as the EMG and to the rectified and filtered signal as the rectified EMG, while others refer to the rectified and filtered signal as the EMG. We take the latter definition and note that, as a practical matter, one typically records only the relatively slowly varying rectified and filtered signal.
6. In the experiments of Carvell *et al.* (1996), the animals were untrained so that only a limited number of trials could be obtained. It may be useful to repeat these measurements with trained animals, as well as use phase-sensitive methods to look for weak correlations.
7. The output of the comparator is a periodic function of the difference between the time dependence of the two input signals, i.e., it is of the form $f\{2\pi\nu_R t - 2\pi\nu_R\tau_D + \phi - (2\pi\nu_D t - 2\pi\nu_D\tau_D)\}$, which equals $f\{2\pi\nu_D(\tau_R - \tau_D) + \phi\}$ at lock. While the periodicity of this function is over an interval of 2π in typical realizations of a phase-sensitive servo, only a periodicity of π is consistent with the data of Ahissar *et al.* (1997). This suggests that the putative neuronal comparator doubles the frequency of the reference from ν_D to $2\nu_D$. A neural mechanism that accomplishes this is a summation of the on- and off-responses from the same oscillatory input.
8. Since different units in vibrissa S1 cortex have different preferred phases (Fig 10), there are presumably multiple copies of the comparator circuit. An alternative possibility is that there is a single comparator circuit that uses a single reference signal that is determined as the vector average of the single unit responses. For the data of Figure 10b, the vector average points toward the retracted but protracting position.

References

Ahissar, E., and S. Haidarliu (1998) Thalamic oscillations compute the phase difference between vibrissal input and barrel cortex oscillations. *Soc. Neurosci. Abstr.* **24**: 151.

Ahissar, E., S. Haidarliu, and M. Zackenhouse (1997) Decoding temporally encoded sensory input by cortical oscillators and thalamic phase comparators. *Proc Natl Acad Sci USA* **94**: 11633–11638.

Ahmed, N., and K.R. Rao (1975) *Orthogonal Transforms for Digital Signal Processing*, Springer, New York.

Andersen, R.A., and V.B. Mountcastle (1983) The influence of angle of gaze upon the excitability of the light sensitive neurons of the posterior parietal cortex. *J Neurosci* **3**: 532–548.

Armstrong-James, M., and K. Fox (1987) Spatiotemporal convergence and divergence in the rat S1 "barrel" cortex. *J Comp Neurol* **263**: 265–281.

Armstrong-James, M., K. Fox, and A. Das-Gupta (1992) Flow of excitability within barrel cortex on striking a single vibrissa. *J Neurophysiol* **68**: 1345–1358.

Aroniadou, V.A., and A. Keller (1993) The patterns and synaptic properties of horizontal intracortical connections in the rat motor cortex. *J Neurophysiol* **70**: 1493–1553.

Arvidsson, J. (1982) Somatotopic organization of vibrissae afferents in the trigeminal sensory nuclei of the rat studied by transganglionic transport of HRP. *J Comp Neurol* **211**: 84–92.

Asanuma, H., and A. Keller (1991) Neural mechanisms of motor learning in mammals. *NeuroReport* **2**: 217–224.

Barneoud, P., M. Gyger, F. Andres, and H. van der Loos (1991) Vibrissa-related behavior in mice: transient effect of ablation of the barrel cortex. *Behav Brain Res* **44**: 87–99.

Belford, G.R., and H.P. Killackey (1979a) The development of vibrissae representation in subcortical trigeminal centers of the neonatal rat. *J Comp Neurol* **188**: 63–74.

Belford, G.R., and H.P. Killackey (1979b) Vibrissa representation in subcortical trigeminal centers of the neonatal rat. *J Comp Neurol* **183**: 305–322.

Benett-Clarke, C.A., N.L. Chiaia, M.F. Jacquin, and R.W. Rhoades (1992) Parvalbumin and calbindin immunocytochemistry reveal functionally distinct cell groups and vibrissa-related patterns in the trigeminal brainstem complex of the adult rat. *J Comp Neurol* **320**: 323–338.

Bermejo, R., D. Houben, and H.P. Zeigler (1996) Conditioned whisking in the rat. *Somatosen Motor Res* **13**: 225–234.

Bowden, R.E.M., and Z.Y. Mahran (1956) The functional significance of the pattern of innervation of the muscle quadratus labii superioris of the rabbit, cat, and rat. *J Anat* **90**: 21–227.

Bower, J.M., D.H. Beerman, J.M. Gibson, G.M. Shambes, and W. Welker (1981) Principles of organization of a cerebro-cerebellar circuit. Micromapping the projections from cerebral (SI) to cerebellar (granule cell layer) tactile areas of rats. *Brain Behav Evol* **18**: 1–18.

Bruce, L.L., J.G. Mchaffie, and B.E. Stein (1987) The organization of trigeminotectal and trigeminothalamic neurons in rodents: a double-labeling study with fluorescent dyes. *J Comp Neurol* **262**: 315–330.

Buzsaki, G. (1991) The thalamic clock: emergent network properties. *Neuroscience* **41**: 351–364.

Cajal, S.R. (1911) *Histologie du Système Nerveux de l'Homme et des Vertébrés*, Maloine, Paris.

Carvell, G.E., S.A. Miller, and D.J. Simons (1996) The relationship of vibrissal motor cortex unit activity to whisking in the awake rat. *Somatosen Motor Res* **13**: 115–127.

Carvell, G.E., and D.J. Simons (1986) Somatotopic organization of the second somatosensory area (SII) in the cerebral cortex of the mouse. *Somatosen Res* **3**: 213–237.

Carvell, G.E., and D.J. Simons (1987) Thalamic and corticocortical connections of the second somatic sensory area of the mouse. *J Comp Neurol* **265**: 409–427.

Carvell, G.E., and D.J. Simons (1990) Biometric analyses of vibrissal tactile discrimination in the rat. *J Neurosci* **10**: 2638–2648.

Carvell, G.E., and D.J. Simons (1995) Task- and subject-related differences in sensorimotor behavior during active touch. *Somatosen Motor Res* **12**: 1–9.

Carvell, G.E., D.J. Simons, S.H. Lichtenstein, and P. Bryant (1991) Electromyographic activity of mystacial pad musculature during whisking behavior in the rat. *Somatosen Motor Res* **8**: 159–164.

Cauller, L.J., and B.W. Connors (1994) Synaptic physiology of horizontal afferents to layer 1 in slices of rat S1 neocortex. *J Neurosci* **14**: 751–762.

Chapin, J.K., M. Sadeq, and J.L.U. Guise (1987) Corticocortical connections within the primary somatosensory cortex of the rat. *J Comp Neurol* **263**: 326–346.

Chapin, J.K., J.S. Schneider, M. Nicolelis, and C.-S. Lin (1990) A major direct GABAergic pathway from zona incerta to neocortex. *Science* **248**: 1553–1556.

Chiaia, N.L., R.W. Rhoades, C.A. Bennett-Clark, S.E. Fish, and H.P. Killackey (1991a) Thalamic processing of vibrissal information in the rat I. Afferent input to the medial ventral posterior and posterior nuclei. *J Comp Neurol* **314**: 201–216.

Chiaia, N.L., R.W. Rhoades, S.E. Fish, and H.P. Killackey (1991b) Thalamic processing of vibrissal information in the rat: II. Morphological and functional properties of medial ventral posterior nucleus and posterior nucleus neurons. *J Comp Neurol* **314**: 217–236.

Clarke, W.B., and D. Bowsher (1962) Terminal distribution of primary afferent trigeminal fibers in the rat. *Exp Neurol* **6**: 372–383.

de Bellescize, H. (1932) La reception synchrone. *Onde Electrique* **11**: 230–240.

Deniau, J.M., H. Kita, and S.T. Kitai (1992) Patterns of termination of cerebellar and basal ganglia efferents in the rat thalamus. Strictly segregated and partly overlapping projections. *Neurosci Lett* **144**: 202–206.

Deschênes, M., J. Bourassa, and A. Parent (1996) Striatal and cortical projections of single neurons from the central lateral thalamic nucleus in the rat. *Neuroscience* **72**: 679–687.

Diamond, M.E. (1995) Somatosensory thalamus of the rat. In *Cerebral Cortex: the Barrel Cortex of Rodents*, E.G. Jones and A. Peters, eds., pp. 189–209, Plenum Press, New York.

Diamond, M.E., M.J. Budway, M. Armstrong-James, and F.F. Ebner (1992) Somatic sensory responses in the rostral sector or the posterior group (POm) and in the ventral posterior medial nucleus (VPM) of the rat thalamus: dependence on the barrel field cortex. *J Comp Neurol* **319**: 66–84.

Dinse, H.R., F. Spengler, K. Kopecz, and G. Schoner (1992) Evoked oscillatory cortical responses are dynamically coupled to peripheral stimuli. *Theoret Neurosci* **3**: 579–582.

Donoghue, J.P., K.L. Kerman, and F.F. Ebner (1979) Evidence of two organizational plans within the somatic sensory-motor cortex of the rat. *J Comp Neurol* **183**: 647–664.

Donoghue, J.P., and S.T. Kitai (1981) A collateral pathway to the neostratum from corticofugal neurons of the rat sensory-motor cortex: an intracellular HRP study. *J Comp Neurol* **201**: 1–13.

Donoghue, J.P., and J.N. Sanes (1988) Organization of adult motor cortex representation patterns following neonatal forelimb nerve injury in rats. *J Neurosci* **8**: 3221–3232.

Dorfl, J. (1982) The musculature of the mystacial vibrissae of the white mouse. *J Anat* **135**: 147–154.

Dorfl, J. (1985) The innervation of the mystacial region of the white mouse. A topographical study. *J Anat* **142**: 173–184.

Drager, U.C., and D.H. Hubel (1976) Topography of visual and somatosensory projections to the mouse superior colliculus. *J Neurophysiol* **39**: 91–101.

Durham, D., and T.A. Woolsey (1977) Barrels and columnar cortical organization: evidence from 2-deoxyglucose (2-DG) experiments. *Brain Res* **137**: 169–174.

Erzurumlu, R.S., and H.P. Killackey (1980) Diencephalic projections of the subnucleus interpolaris of the brainstem trigeminal complex in the rat. *Neuroscience* **5**: 1891–1901.

Erzurumlu, R.S., and H.P. Killackey (1979) Efferent connections of the brainstem trigeminal complex with the facial nucleus of the rat. *J Comp Neurol* **188**: 75–86.

Fabri, M., and H. Burton (1991a) Ipsilateral cortical connections of primary somatic sensory cortex in rats. *J Comp Neurol* **311**: 405–424.

Fabri, M., and H. Burton (1991b) Topography connections between primary somatosensory cortex and posterior complex in rat: a multiple fluorescent tracer study. *Brain Res* **538**: 351–357.

Faull, R.L.M., and W.R. Mehler (1978) The cells of origin of nigrotectal, nigrothalamic and nigrostriatal projections in the rat. *Neuroscience* **3**: 989–1002.

Fee, M.S., P.P. Mitra, and D. Kleinfeld (1996) Automatic sorting of multiple unit neuronal signals in the presence of anisotropic and non-Gaussian variability. *J Neurosci Meth* **69**: 175–188.

Fee, M.S., P.P. Mitra, and D. Kleinfeld (1997) Central versus peripheral determinates of patterned spike activity in rat vibrissa cortex during whisking. *J Neurophysiol* **78**: 1144–1149.

Gerfen, C.R., W.A. Staines, G.W. Arbuthnott, and H.C. Fibiger (1982) Crossed connections of the substantia nigra in the rat. *J Comp Neurobiol* **207**: 283–303.

Getting, P.A. (1989) Emerging principles governing the operation of neural networks. *Ann Rev Neurosci* **12**: 185–204.

Gioanni, Y., and M. Lamarche (1985) A reappraisal of rat motor cortex organization by intracortical microstimulation. *Brain Res* **344**: 49–61.

Goldreich, D., T.L. Prigg, G.E. Carvell, and D.J. Simons (1997) Neurophysiological recordings during a computer-automated vibrissal tactile discrimination task. *Soc. Neurosci. Abstr.* **23**: 23.

Guic-Robles, E., W.M. Jenkins, and H. Bravo (1992) Vibrissal roughness discrimination is barrel cortex-dependent. *Behav Brain Res* **48**: 145–152.

Guic-Robles, E., C. Valdivieso, and G. Guajardo (1989) Rats can learn a roughness discrimination using only their vibrissal system. *Behav Brain Res* **31**: 285–289.

Hall, R.D., and E.P. Lindholm (1974) Organization of motor and somatosensory neocortex in the albino rat. *Brain Res* **66**: 23–38.

Haroian, A.J., L.C. Massopust, and P.A. Young (1981) Cerebellothalamic projections in the rat: an autoradiographic and degeneration study. *J Comp Neurol* **197**: 217–236.

Hoogland, P.V., E. Welker, and H. Van der Loos (1987) Organization of the projections from barrel cortex to thalamus in mice studied with *Phaseolus vulgaris*-leucoagglutinin and HRP. *Exp Brain Res* **68**: 73–87.

Huerta, M., A. Frankfurter, and J. Harting (1983) Studies of the principal sensory and spinal trigeminal nuclei of the rat: projections to the superior colliculus, inferior olive, and cerebellum. *J Comp Neurol* **220**: 147–167.

Hutson, K.A., and R.B. Masterton (1986) The sensory contribution of a single vibrissa's cortical barrel. *J Neurophysiol* **56**: 1196–1223.

Isokawa-Akesson, M., and B.R. Komisaruk (1987) Difference in projections to the lateral and medial facial nucleus: anatomically separate pathways for rhythmical vibrissa movement in rats. *Exp Brain Res* **65**: 385–398.

Izraeli, R., and L.L. Porter (1995) Vibrissal motor cortex in the rat: connections with the barrel field. *Exp Brain Res* **104**: 41–54.

Jacquin, M., M, Barcia, and R.W. Rhoades. (1989) Structure–function relationships in rat brainstem subnucleus interpolaris: IV. Projection neurons. *J Comp Neurol* **282**: 45–62.

Jacquin, M.F., N.L. Chiaia, J.H. Haring, and R.W. Rhoades (1990a) Intersubnuclear connections within the rat trigeminal brainstem complex. *Somatosen Motor Res* **7**: 399–420.

Jacquin, M.F., M.R. Wiegand, and W.E. Renehan (1990b) Structure–function relationships in rat brain stem subnucleus interpolaris. VIII. Cortical inputs. *J Neurophysiol* **64**: 3–27.

Kam, Z., H.B. Shore, and G. Feher (1975) Simple schemes for measuring autocorrelation functions. *Rev Scientif Instr* **46**: 269–277.

Kamen, G., and G.E. Caldwell (1996) Physiology and interpretation of the electromyogram. *J Clin Neurophysiol* **13**: 366–384.

Kassel, J. (1980) Superior colliculus projections to tactile areas of rat verebellar hemispheres. *Brain Res* **202**: 291–305.

Keller, A. (1993) Intrinsic synaptic organization of the motor cortex. *Cerebral Cortex* **3**: 430–441.

Keller, A. (1995) Synaptic organization of the barrel cortex. In *Cerebral Cortex: the Barrel Cortex of Rodents*, E.G. Jones and A. Peters, eds., pp. 221–262, Plenum Press, New York.

Kennedy, T.T., R.J. Grimm, and A.L. Towe (1966) The role of cerebral cortex in evoked somatosensory activity in cat cerebellum. *Exp Neurol* **14**: 13–32.

Killackey, H., and R. Erzurumlu (1981) Trigeminal projections to the superior colliculus of the rat. *J Comp Neurol* **201**: 221–242.

Killackey, H.P., M. Jacquin, and R.W. Rhoades (1990) Development of somatosensory system structures. In *Development of Sensory Systems in Mammals*, J.R. Coleman, ed., pp. 403–429, John Wiley, New York.

Kim, U., E. Gregory, and W.C. Hall (1992) Pathway from the zona incerta to the superior colliculus in the rat. *J Comp Anat* **321**: 555–575.

Kleinfeld, D., and K.R. Delaney (1996) Distributed representation of vibrissa movement in the upper layers of somatosensory cortex revealed with voltage sensitive dyes. *J Comp Neurol* **375**: 89–108.

Kleinfeld, D., and H. Sompolinsky (1988) Associative neural network model for the generation of temporal patterns: theory and application to central pattern generators. *Biophys J* **54**: 1039–1051.

Koch, C., and T. Poggio (1992) Multiplying with synapses and neurons. In *Single Neuron Computation*, T. McKenna, J. Davis, and S.F. Zornetzer, eds., pp. 315–345, Academic Press, Boston.

Kolmac, C.I., B.D. Power, and J. Mitrofanis (1998) Patterns of connections between zona incerta and brainstem in rats. *J Comp Neurol* **396**: 544–555.

Koralek, K., K.F. Jensen, and H.P. Killackey (1988) Evidence for two complementary patterns of thalamic input to the rat somatosensory cortex. *Brain Res* **463**: 346–351.

Lee, H.S., R.J. Kosinski, and G.A. Mihailoff (1989) Collateral branches of cerebellopontine axons reach the thalamus, superior colliculus, or inferior olive: a double-fluorescence and combined fluorescence-horseradish peroxidase study in the rat. *Neuroscience* **28**: 725–734.

Lévesque, M., A. Charara, S. Gagnon, A. Parent, and M. Deschênes (1996) Corticostriatal projections from layer V cells in rat are collaterals of long-range corticofugal axons. *Brain Res* **709**: 311–315.

LUND, R.D., and K.E. WEBSTER (1967) Thalamic afferents from the spinal cord and trigeminal nuclei. *J Comp Neurol* **130**: 313–328.

MA, P.K.M., and T.A. WOOLSEY (1984) Cytoarchitectural correlates of vibrissae in the medullary trigeminal complex of the mouse. *Brain Res* **306**: 374–379.

MANTLE-ST. JOHN, L.A., and D.J. TRACEY (1987) Somatosensory nuclei in the brainstem of the rat: independent projections to the thalamus and cerebellum. *J Comp Neurol* **255**: 259–271.

MARTIN, M.R., and D. LODGE (1977) Morphology of the facial nucleus of the rat. *Brain Res* **38**: 206–210.

MCCORMICK, D.A., and T. BAL (1997) Sleep and arousal: thalamocortical mechanisms. *Ann Rev Neurosci* **20**: 185–215.

MERCIER, B.E., C.R. LEGG, and M. GLICKSTEIN (1990) Basal ganglia and cerebellum receive different somatosensory information in rats. *Proc Natl Acad Sci USA* **87**: 4388–4392.

MIDDLETON, F.A., and P.L. STRICK (1997) Cerebellar output channels. *Int Rev Neurobiol* **41**: 61–82.

MIYASHITA, E., A. KELLER, and H. ASANUMA (1994) Input–output organization of the rat vibrissal motor cortex. *Exp Brain Res* **99**: 223–232.

MIYASHITA, E., and M. SHIGEMI (1995) The superior colliculus relays signals descending from the vibrissal motor cortex to the facial nerve nucleus in the rat. *Neurosci Lett* **195**: 69–71.

MOGOSEANU, D., A.D. SMITH, and J.P. BOLAM (1994) Monosynapatic innervation of facial motoneurones by neurones of the parvicellular reticular formation. *Exp. Brain Res.* **101**: 427–438.

MORISETTE, J., and J.M. BOWER (1996) Contribution of somatosensory cortex to responses in the rat cerebellum granule cell layer following peripheral tactile stimulation. *Exp Brain Res* **109**: 240–250.

MOXON, K.A., R.S. MARKOWITZ, and J.K. CHAPIN (1998) Neural ensemble activity during a whisker discrimination task: sensory modulation at different levels of the trigeminal system. *Soc. Neurosci. Abstr.* **24**: 133.

NAKAJIMA, S., Y. KOMATSU, and K. TOYAMA (1988) Synaptic action of layer 1 fibers on cells in cat striate cortex. *Brain Res* **457**: 176–180.

NEAFSEY, E.J., E.L. BOLD, G. HAAS, K.M. HURLEY-GIUS, G. QUIRK, C.F. SIEVERT, and R.R. TERREBERRY (1986) The organization of the rat motor cortex: a microstimulation mapping study. *Brain Res Rev* **11**: 77–96.

NICOLELIS, M.A., A.A. GHAZANFAR, B.M. FAGGIN, S. VOTAW, and L.M. OLIVEIRA (1997) Reconstructing the engram: simultaneous, multisite, many single neuron recordings. *Neuron* **18**: 529–537.

NICOLELIS, M.A.L., L.A. BACCALA, R.C.S. LIN, and J.K. CHAPIN (1995) Sensorimotor encoding by synchronous neural ensemble activity at multiple levels of the somatosensory system. *Science* **268**: 1353–1358.

NICOLELIS, M.A.L., J.K. CHAPIN, and R.C.S. LIN (1992) Somatotopic maps within the zona incerta relay parallel GABAergic somatosensory pathways to the neocortex, superior colliculus, and brainstem. *Brain Res* **577**: 134–141.

NICOLELIS, M.A.L., R.C.S. LIN, D.J. WOODWARD, and J.K. CHAPIN (1993) Dynamic and distributed properties of many-neuron ensembles in the ventral posterior medial thalamus of awake rats. *Proc Natl Acad Sci USA* **90**: 2212–2216.

NIEMI-JUNKOLA, U.J., and G.W.M. WESTBY (1998) Spatial variation in the effects of inactivation of substantia nigra on neuronal activity in rat superior colliculus. *Neurosci Lett* **241**: 175–179.

NOTHIAS, F., M. PESCHANSKI, and J.-M. BESSON (1988) Somatotopic reciprocal connections between the somatosensory cortex and thalamic Po nucleus in rat. *Brain Res* **447**: 169–174.

NOZAKI, S., A. IRIKI, and Y. NAKAMURA (1986) Location of central rhythm generator involved in cortically induced rhythmical masticatory jaw-opening movement in the guinea pig. *J Neurophysiol* **55**: 806–825.

PAPEZ, J.W. (1927) Subdivisions of the facial nucleus. *J Comp Neurol* **42**: 159–191.

POWER, B.D., C.I. KOLMAC, and J. MITROFANIS (1999) Evidence for a large projection from the zona incerta to the dorsal thalamus. *J Comp Neurol* **404**: 554–565.

RICE, F.L., and J. ARVIDSSON (1991) Central projections of primary sensory neurons innervating different parts of the vibrissae follicles and intervibrissal skin on the mystacial pad of the rat. *J Comp Neurol* **309**: 1–16.

RICE, F.L., B.T. FUNDIN, K. PFALLER, and J. ARVIDSSON (1994) The innervation of the mystacial pad in the adult rat studied by anterograde transport of HRP conjugates. *Exp Brain Res* **99**: 233–246.

RICE, F.L., A. MANCE, and B.L. MUNGER (1986) A comparative light microscopic analysis of the sensory innervation of the mystacial pad. I. Innervation of vibrissal follicle–sinus complexes. *J Comp Neurol* **252**: 154–174.

SACHDEV, R.N.S., E.W. JENKINSON, and F.F. EBNER (1998) Response properties of barrel field neurons in awake, behaving rat. *Soc. Neurosci. Abstr.* **24**: 633.

SANES, J.N., S. SUNER, and J.P. DONAHUE (1990) Dynamic organization of primary motor cortex output to target muscles in adult rats II. Long-term patterns of reorganization following motor or mixed peripheral nerve lesions. *Exp Brain Res* **79**: 479–491.

SEMBA, K., and B.R. KOMISARUK (1984) Neural substrates of two different rhythmical vibrissal movements in the rat. *Neuroscience* **12**: 761–774.

SHAMBES, G.M., J.M. GIBSON, and W. WELKER (1978) Fractured somatotopy in granule cell tactile areas of rat cerebellar hemispheres revealed by micromapping. *Brain Behav Evol* **15**: 94–140.

SIMONS, D.J. (1978) Response properties of vibrissal units in rat S1 somatosensory neocortex. *J Neurophysiol* **41**: 798–820.

SIMONS, D.J., G.E. CARVELL, and S.H. LICHTENSTEIN (1990) Responses of rat trigeminal ganglion neurons to movements of vibrissae in different directions. *Somatosen Motor Res* **7**: 47–65.

SIMONS, D.J., and J.A. HARTINGS (1998) Thalamic relay of afferent responses to 1- to 12-Hz whisker stimulation in the rat. *J Neurophysiol* **80**: 1016–1019.

SMITH, R.L. (1973) The ascending fiber projections from the principal sensory trigeminal nucleus in the rat. *J Comp Neurol* **148**: 423–446.

STEIN, B.E., B. MAGALHAES-CASTRO, and L. KRUGER (1975) Superior colliculus: visuotopic–somatotopic overlap. *Science* **189**: 224–225.

STEINDLER, D.A. (1985) Trigeminocerebellar, trigeminotectal, and trigeminothalamic projections: a double retrograde axonal tracing study in the mouse. *J Comp Neurol* **237**: 155–175.

STERIADE, M., D.A. MCCORMICK, and T.J. SEJNOWSKI (1993) Thalamocortical oscillations in the sleeping and aroused brain. *Science* **262**: 679–685.

SUGITANI, M., J. YANO, T. SUGAI, and H. OOYAMA (1990) Somatopic organization and columnar structure of the vibrissae representation in the rat ventrobasal complex. *Exp Brain Res* **81**: 346–351.

SWENSON, R.S., R.J. KOSINSKI, and A.J. CASTRO (1984) Topography of spinal, dorsal column nuclear, and spinal trigeminal projections to the pontine gray in rats. *J Comp Neurol* **222**: 301–311.

Tokuno, H., M. Takada, Y. Ikai, and N. Mizuno (1994) Direct projections from the deep layers of the superior colliculus to the subthalamic nucleus in the rat. *Brain Res* **639**: 156–160.

Torvik, A. (1956) Afferent connections to the sensory trigeminal nuclei, the nucleus of the solitary tract and adjacent structures. An experimental study in the rat. *J Comp Neurol* **106**: 51–132.

Van Der Loos, H. (1976) Barreloids on the mouse somatosensory thalamus. *Neurosci Lett* **2**: 1–6.

Vincent, S.B. (1912) The function of the vibrissae in the behavior of the white rat. *Behav Monogr* **1**: 7–81.

Vincent, S.B. (1913) The tactile hair of the white rat. *J Comp Neurol* **23**: 1–23.

Watson, C.R.R., and R.C. Switzer III (1978) Trigeminal projections to cerebellar tactile areas in the rat. Origin mainly from n. interpolaris and n. principalis. *Neurosci Lett* **10**: 77–82.

Weiss, D.S., and A. Keller (1994) Specific patterns of intrinsic connections between representation zones in the rat motor cortex. *Cerebral Cortex* **4**: 205–214.

Welker, C. (1976) Receptive fields of barrels in the somatosensory neocortex of the rat. *J Comp Neurol* **166**: 173–190.

Welker, E., P.V. Hoogland, and H. van der Loos (1988) Organization of feedback and feedforward projections of the barrel cortex: A PHA-L study in the mouse. *Exp Brain Res* **73**: 411–435.

Welker, W.I. (1964) Analysis of sniffing of the albino rat. *Behaviour* **12**: 223–244.

Welsh, J.P., E.J. Lang, I. Suglhara, and R. Llinas (1995) Dynamic organization of motor control within the olivocerebellar system. *Nature* **374**: 453–457.

Westby, G.W., C. Collinson, and P. Dean (1993) Excitatory drive from deep cerebellar neurons to the superior colliculus in the rat: an electrophysiological mapping study. *Eur J Neurosci* **5**: 1378–1388.

Westby, G.W., C. Collinson, P. Redgrave, and P. Dean (1994) Opposing excitatory and inhibitory influences from the cerebellum and basal ganglia converge on the superior colliculus: an electrophysiological investigation in the rat. *Eur J Neurosci* **6**: 1335–1342.

White, E.L., and R.A. Deamicis (1977) Afferent and efferent projections of the region in mouse Sml cortex which contain the posteromedial barrel subfield. *J Comp Neurol* **175**: 455–482.

Wiesendanger, R., and M. Wiesendanger (1982a) The corticopontine system in the rat. I. Mapping of corticopontine neurons. *J Comp Neurol* **208**: 215–226.

Wiesendanger, R., and M. Wiesendanger (1982b) The corticopontine system in the rat. II. The projection pattern. *J Comp Neurol* **208**: 227–238.

Williams, M.N., D.S. Zahm, and M.F. Jacquin (1994) Differential foci and synaptic organization of the principal and spinal trigeminal projections to the thalamus in the rat. *Eur J Neurosci* **6**: 429–453.

Wineski, L.E. (1983) Movements of the cranial vibrissae in the golden hamster (*Mesocritus auratus*). *J Zool* (*Lond*) **200**: 261–280.

Wineski, L.E. (1985) Facial morphology and vibrissal movement in the golden hamster. *J Morphol* **183**: 199–217.

Wise, S.P., and E.G. Jones (1977) Cells of origin and terminal distribution of descending projections of the rat somatic sensory cortex. *J Comp Neurol* **175**: 129–158.

Woolsey, T.A., C. Welker, and R.H. Schwartz (1974) Comparative anatomical studies of the SmI face cortex with special reference to the occurrence of "barrels" in layer IV. *J Comp Neurol* **164**: 79–94.